

Stochastic Integrate and Fire Models: a review on mathematical methods and their applications

Laura Sacerdote and Maria Teresa Giraudo

Abstract

Mathematical models are an important tool for neuroscientists. During the last thirty years many papers have appeared on single neuron description and specifically on stochastic Integrate and Fire models. Analytical results have been proved and numerical and simulation methods have been developed for their study. Reviews appeared recently collect the main features of these models but do not focus on the methodologies employed to obtain them. Aim of this paper is to fill this gap by upgrading old reviews on this topic. The idea is to collect the existing methods and the available analytical results for the most common one dimensional stochastic Integrate and Fire models to make them available for studies on networks. An effort to unify the mathematical notations is also made. This review is divided in two parts:

1. Derivation of the models with the list of the available closed forms expressions for their characterization;
2. Presentation of the existing mathematical and statistical methods for the study of these models.

Laura Sacerdote and Maria Teresa Giraudo

Department of Mathematics, University of Torino, Via Carlo Alberto 10 Torino, Italy e-mail: laura.sacerdote@unito.it, mariateresa.giraudo@unito.it

Work supported by MIUR PRIN 2008. LS is grateful to the organizers of the Summer School "Stochastic Differential Equation Models with Applications to the Insulin-Glucose System and Neuronal Modelling" for their kind hospitality.

1 Introduction

Progresses in experimental techniques, with the possibility to record simultaneously from many neurons, move the interest of scientists from single neuron to small or large networks models. Hence the time seems ripe to summarize the contribution of single neuron models to our knowledge of neuronal coding. Various types of spiking neuron models exist, with different levels of details in the description. They range from biophysical ones on the lines of the classic paper of 1952 by Hodgkin and Huxley [65], to the "integrate and fire" variants (see for example [42], [64], [99]). Integrate and Fire (IF) type models disregard biological details, that are accounted for through a stochastic term, to focus on causal relationships in neuronal dynamics. Their relative simplicity make them good candidates for the study of networks. Recent reviews discuss qualitative (cf. [18], [19]) and quantitative (cf. [70]) features of stochastic Leaky Integrate and Fire (LIF) models. These models are a variant of IF models where the spontaneous membrane decay is introduced. An older paper ([107]) concerns mathematical methods for their study. The aim of this work is to collect the existing mathematical methods for LIF models, to provide a set of methodologies for future studies on networks. Indeed, although the stochastic LIF models are simplified representations of the cells, they are considered good descriptors of the neuron spiking activity (cf. for example [69], [73]). Though some criticisms have appeared, showing some lacks in the fit of experimental data (cf. [70]), these models are still largely employed. The most used is the Ornstein-Uhlenbeck (OU) version but all of them have played a role for the understanding of the mechanisms involved in neuronal code

The first IF models date back to 1907, when Lapique ([87]) proposed to describe the membrane potential evolution of a neuron, subject to an input, using the time derivative of the law for the capacitance. In the presence of an input current, the membrane voltage increases until it reaches a constant threshold S . Then a spike occurs and the voltage is reset to its resting value, to start again to evolve (cf. [134]). Although it reasonably fitted some experimental data this model lied disregarded till the second half of the last century. Then it became the embrional idea for "integrate and fire" models. The leading idea in the formulation of stochastic IF and LIF models was to

partition the features of the neuron in two groups: the first ones were accounted for by the mathematical description of the neuronal (deterministic) dynamics and the second ones globally considered by means of a noise term. In Sect. 3 we derive the most popular LIF models after a brief description of the biological features of interest in Sect. 2.

Improvements of LIF models were proposed in the eighties, following the initial illusion to become able to recognize the main laws governing our brain. The lack of suitable mathematical instruments made soon clear the difficulty to determine explicit expressions for the input-output relationship. The end of the eighties and the starting years of the nineties are characterized by mathematical and numerical advances, accompanied by the development of new faster computers. Section 4 is devoted to a review of the main mathematical methods for the study of stochastic LIF models, updating previous reviews [1], [105] and [107].

In the nineties the use of such methodologies, as well as specific reliable and powerful simulation methods, allowed to obtain a deeper knowledge of the models' features. Unexpected results on the role of noise in neuronal coding have been proved mathematically and confirmed experimentally (cf. for example [128]).

Surprisingly, all research on LIF models has disregarded for a long time their ability to fit real data. The only exception was [77] that considered the parameter estimation problem. Recently papers on the statistical estimation of model parameters started to appear. Section 5 is dedicated to this subject.

2 Biological features of the neuron

A comprehensive description of the physiological properties of neurons is outside the aims of this work. We refer to [134], [135] and [42] for an exhaustive exposition of neurobiological properties relevant in the modeling context.

The neurons are the elementary processing units in the central nervous system, interconnected with intricate patterns. Neurons of different sizes and shape, but sharing some fundamental features, exist in all the areas of the brain. Their estimated number in the human brain is around 10^{12} . A typical neuron can be divided into three distinct parts called dendrites, axon and

soma. The dendrites play the role of the input device collecting signals from other neurons and transmitting them to the soma. The soma is the non-linear processing unit of the neuron. It generates a signal, known as spike or action potential, if the total amount of inputs exceeds a certain threshold. The axon is the output device carrying the signal to the other neurons.

The action potentials are electrical pulses, having a duration of about $1-2$ *ms* and an amplitude of around 100 *mV*. They do not change their shape along the transmission. A neuron cannot elicit a second spike immediately after a first one has occurred due to the presence of a refractory period. A chain of action potentials emitted by a single neuron is called a spike train, a series of similar events occurring either at regularly spaced instants of time or more randomly. The time between two consecutive spikes is called interspike interval (ISI).

The site where the axon of a presynaptic neuron is linked with the dendrite or the soma of a postsynaptic cell is the synapse, which often in the vertebrates is of chemical type. When an action potential reaches a synapse, it triggers complex bio-chemical reactions leading to the release of a neurotransmitter and the opening of specific ionic channels on the membrane. The ion influx leads to a change in the potential value at the postsynaptic site and the translation of the chemical signal into an electrical one. This voltage response is called the postsynaptic potential (PSP).

The effect of a spike on the postsynaptic neuron is measured in terms of the potential difference between the interior of the cell and its surroundings, called membrane potential. In the absence of spike inputs, the cell is at a resting level of about -65 *mV*. If the change in membrane potential is positive the synapse is excitatory and induces a negative depolarization, otherwise it is inhibitory and hyperpolarizes the cell. In the absence of inputs, i.e. in the silent state, the neuron membrane potential decays exponentially toward the resting level.

The dimensions and number of synapses vary for different neurons. Some neurons, such as Purkinje cerebellar cells, pyramidal neurons and interneurons recorded in vitro (cf. for example [70]), have a huge number of synapses and extended dendritic trees. Integrate and fire models can then be employed for the description of their output behavior since, due to the large number of synapses, limit theorems can be used (cf. [70], [101]).

3 One dimensional Stochastic Integrate and Fire Models

3.1 Introduction and Notations

The huge number of synapses impinging on the neuron determines a stochasticity in the activating current not considered in the Lapique model. The first attempt to formulate a stochastic IF model is due to Gerstein and Mandelbrot. In [41] they fitted a number of recorded ISI's through the Inverse Gaussian (IG) distribution, i.e. the first passage time distribution of a Wiener process through a constant boundary S . They described the membrane potential dynamics preceding the release of a spike through a Wiener process. To get a renewal process they assumed that after each spike the membrane potential is instantaneously reset to its initial value (cf. for example [27] for an introduction on these processes). This model is the basis of successive more realistic models.

In the models, classified as stochastic IF or LIF, one describes the time evolution of the membrane potential by means of a suitable stochastic process $X = \{X_t, t > t_0\}$ with $X_{t_0} = x_0$ and identifies the ISI's with the random variable (r.v.) first passage time (FPT) of X through the threshold S :

$$T = T_S = \inf \{t > t_0 : X_t > S\}. \quad (1)$$

The probability density function (pdf) of T , when it exists, is

$$g(t) = g(S, t | x_0, t_0) = \frac{\partial}{\partial t} P(T < t). \quad (2)$$

When $t_0 = 0$ we simply write $g(S, t | x_0)$. In some instances $S = S(t)$.

In Subsections 3.2, 3.5 and 3.6 we focus on models that describe the sub-threshold membrane potential as a diffusion process. In Subsects. 3.3 and 3.4 we present two continuous time Markov models, the Randomized Random Walk and Stein's model. Reviews on IF and LIF models have already appeared (cf. [105], [107], [82]) but here we unify the notations and we list in a single contribution the mathematical results sparse in different papers.

In the case of models using a diffusion process $X = \{X_t, t > t_0\}$, the diffusion interval is $I = (l, r)$, the drift coefficient and infinitesimal variance (the infinitesimal moments) are:

$$\begin{aligned}\mu(x) &= \lim_{\Delta t \rightarrow 0} \frac{1}{\Delta t} E(\Delta X_t | X_t = x) \\ \sigma^2(x) &= \lim_{\Delta t \rightarrow 0} \frac{1}{\Delta t} E((\Delta X_t)^2 | X_t = x),\end{aligned}\tag{3}$$

with $\Delta X_t = X_{t+\Delta t} - X_t$. The transition pdf $f(x, t | x_0, t_0) = \frac{\partial P(X_t \leq x | X_{t_0} = x_0)}{\partial x}$ is solution of the Kolmogorov equation (cf. [101]):

$$\frac{\partial f(x, t | x_0, t_0)}{\partial t_0} + \mu(x_0) \frac{\partial f(x, t | x_0, t_0)}{\partial x_0} + \frac{\sigma^2(x_0)}{2} \frac{\partial^2 f(x, t | x_0, t_0)}{\partial x_0^2} = 0\tag{4}$$

and of the Fokker-Planck equation

$$\frac{\partial f(x, t | x_0, t_0)}{\partial t} = -\frac{\partial}{\partial x} \{ \mu(x) f(x, t | x_0, t_0) \} + \frac{1}{2} \frac{\partial^2}{\partial x^2} \{ \sigma^2(x) f(x, t | x_0, t_0) \}\tag{5}$$

with initial delta condition

$$\lim_{t_0 \rightarrow t} f(x, t | x_0, t_0) = \delta(x - x_0).\tag{6}$$

Here δ denotes the Dirac delta function.

We suppose that the infinitesimal moments verify some mild conditions (cf. [72], [101], [107]) to guarantee the existence of the solutions of the Fokker-Planck and Kolmogorov equations. Furthermore, when a dependence of the diffusion coefficients from t is not specified, the processes are time homogeneous, i.e. their properties are invariant with respect to time shifts. When eq. (4) is solved in the presence of an absorbing boundary in $x = S$, a further absorption condition must be imposed:

$$\lim_{x \rightarrow S} f^a(x, t | x_0, t_0) = 0.\tag{7}$$

where $f^a(x, t | x_0, t_0) = \frac{\partial}{\partial x} P(X_t < x, T_S > t | X_s = y)$ is the corresponding transition pdf. To get renewal processes, X is always reset to x_0 after each spike.

To characterize a diffusion model, one can also make use of the Ito-type stochastic differential equation (SDE) verified by the process (cf. **SU-SANNE**).

Jump diffusion models, allowing to distinguish the effect of neuronal inputs according with their frequency and their size, are presented in Subsection 3.8.

The role of the threshold shape is illustrated in Subsect. 3.9, and the most recently introduced IF models are surveyed in Subsection 3.10.

To switch from the description of the spike times of the neuron to the count of the number of spikes up to a given time t , we introduce, in Subsection 3.11, the return processes.

3.2 Wiener Process Model

Gerstein and Mandelbrot (cf. [41]) described the time evolution of the sub-threshold membrane potential through a Wiener process \overline{W}_t characterized by infinitesimal moments

$$\mu(x) = \mu \quad \sigma^2(x) = \sigma^2 \quad (8)$$

with $\mu \in \mathbb{R}$, $\sigma > 0$. Their model was motivated by experimental observations of the ISI's exhibiting histograms typical of stable distributions. Indeed this property is exhibited by the FPT of a Wiener process. One gets such process from the standard Wiener process W (cf. **SUSANNE**) through the transformation

$$\overline{W}_t = \mu t + \sigma W_t; \forall t \geq 0. \quad (9)$$

To relate the use of the Wiener process with the membrane potential evolution, Gerstein and Mandelbrot observed that the Wiener process is the continuous limit of a random walk (cf. **SUSANNE**). The occurring of jumps models the incoming of PSP's. The continuous limit is a good approximation when the inputs are of small size and frequent. The transition pdf of W is

$$\begin{aligned} f_W(x, t | x_0, t_0) &\equiv \frac{\partial P(W_t < x | W_{t_0} = x_0)}{\partial x} & (10) \\ &= \frac{1}{\sqrt{2\pi\sigma^2(t-t_0)}} \exp \left\{ -\frac{[x - x_0 - \mu(t-t_0)]^2}{2\sigma^2(t-t_0)} \right\}. \end{aligned}$$

To mimic the spiking times a constant absorbing boundary S is introduced. The spike times are then identified with the FPT, T , of the Wiener process originated at $W_{t_0} = x_0$ through the boundary. To obtain the renewal property, the process is instantaneously reset at x_0 after each spike. Hence the ISI's correspond to the iid r.v.'s T_n , $n = 1, 2, \dots$, with $T_n \sim T$.

The transition pdf of W , if $W_{t_0} = x_0$ is Gaussian with mean $E(W_t) = x_0 + \mu t$ and variance $Var(W_t) = \sigma^2 t$, while the FPT pdf through a constant boundary $S > x_0$ is an IG distribution, hence the pdf and the cumulative distribution are:

$$g(S, t | x_0) = \frac{S - x_0}{\sqrt{2\pi\sigma^2 t^3}} \exp\left\{-\frac{(S - x_0 - \mu t)^2}{2\sigma^2 t}\right\}; \quad (11)$$

$$P(T < t) = \frac{1}{2} \left\{ \operatorname{Erfc}\left[\frac{S - x_0 - \mu t}{\sigma\sqrt{2t}}\right] + e^{\frac{2\mu(S - x_0)}{\sigma^2}} \operatorname{Erfc}\left[\frac{S - x_0 + \mu t}{\sigma\sqrt{2t}}\right] \right\}. \quad (12)$$

Here Erfc denotes the complementary error function (cf. [2]). The mean value and the variance of the FPT are

$$E(T) = \frac{S - x_0}{\mu}; \quad Var(T) = \frac{(S - x_0)\sigma^2}{\mu^3}. \quad (13)$$

The transition pdf in the presence of a constant absorbing boundary S is (cf. [105]):

$$f^a(x, t | y, s) = \frac{1}{\sigma\sqrt{2\pi(t-s)}} \left(\exp\left[-\frac{(x - y - \mu(t-s))^2}{2\sigma^2(t-s)}\right] - \exp\left[\frac{2\mu}{\sigma^2}(S - y) - \frac{(x - 2S + y - \mu(t-s))^2}{2\sigma^2(t-s)}\right] \right). \quad (14)$$

Despite the excellent fitting with some experimental data, Gerstein and Mandelbrot model was criticized for its biological simplifications (cf. [135]). However it allows to obtain results that help the intuition for more realistic models and it is still used for this aim, taking advantage of the existence of a closed form FPT pdf through a constant boundary.

Its FPT pdf is known also through particular time dependent boundaries. These FPT's can be used to account for the refractory period following a spike. Indeed a time varying boundary, assuming high values at small times

and then decreasing, makes short ISI's rare. The FPT pdf is known for a continuous piecewise-linear boundary $S(t) = \alpha_i + \beta_i t, : t \in [t_{i-1}, t_i], : i \geq 1$ where $t_0 < t_1 < t_2 < \dots$ and $\alpha_i, \beta_i \in \mathbb{R}$ with $t_0 \geq 0$. If $t \in [0, \infty)$, such boundary is linear and the FPT pdf is

$$g(\alpha_1 + \beta_1 t, t | x_0) = \frac{|\alpha_1 - x_0|}{\sigma \sqrt{2\pi t^3}} \exp - \frac{[\alpha_1 + \beta_1 t - \mu t - x_0]^2}{2\sigma^2 t}. \quad (15)$$

In the general case, setting $\alpha_{i+1} = \alpha_i + \beta_i t_i$ one gets that $t \mapsto S(t)$ is continuous on $[t_0, \infty)$. If we put $S_i = S(t_i)$, the transition pdf for the process W in the presence of absorbing boundary $S(t)$, $f^a(x_1, t_1; x_2, t_2; \dots; x, t | x_0, t_0)$, is for $t \in (t_{n-1}, t_n)$ (cf. [137]):

$$\begin{aligned} f^a(x_1, t_1; x_2, t_2; \dots; x, t | x_0, t_0) &= \frac{\partial^n}{\partial x_1 \dots \partial x_n} \quad (16) \\ \{P(W_{t_1} < x_1, \dots, W_{t_{n-1}} < x_{n-1}, W_t < x; T > t | W_{t_0} = x_0 < \alpha_1)\} \\ &\times \prod_{i=1}^{n-1} f^a(x_i, t_i | x_{i-1}, t_{i-1}) f^a(x, t | x_{n-1}, t_{n-1}) \\ &\times \prod_{i=1}^{n-1} \left(1 - e^{-2 \frac{(S_i - x_i)(S_{i-1} - x_{i-1})}{t_i - t_{i-1}}} \right) \\ &\times \frac{f^a(x, t | x_{n-1}, t_{n-1})}{\sqrt{2\pi(t_i - t_{i-1})}} \exp \left(- \frac{(x_i - x_{i-1})^2}{2(t_i - t_{i-1})} \right) \end{aligned}$$

for $x_i \leq S_i, 1 \leq i \leq n; x_0 < S_0$ and $x \in (-\infty, S)$.

Further closed form expressions for the FPT of a Wiener process have been obtained by the method of images (cf. [29]) or as solutions of suitable integral equations ([104]), when $\left| \frac{dS(t)}{dt} \right| \leq C t^{-\alpha}$, with $\alpha < 1/2$ and C a constant. This last case is discussed in Section 4.1.1. and involves series of multiple integrals.

3.3 Randomized Random Walk Model

In the Randomized Random Walk (RRW) the regularly spaced intertimes of the random walk between PSPs are substituted with exponentially distributed intertimes of parameters λ^+ and λ^- for excitatory and inhibitory PSP's respectively. The process X with $X_0 = 0$ has mean and variance

$$E(X_t) = \delta(\lambda^+ - \lambda^-)t; \quad Var(X_t) = \delta^2(\lambda^+ + \lambda^-)t, \quad (17)$$

respectively. Here $\delta > 0$ is the constant amplitude of PSP's. The FPT pdf through the boundary S , with S an integer multiple of δ , is (cf. [135]):

$$g(S, t|0) = \frac{S}{\delta} \left(\frac{\lambda^+}{\lambda^-} \right)^{S/2\delta} \frac{e^{-(\lambda^+ + \lambda^-)t}}{t} I_{S/\delta} \left(2t\sqrt{\lambda^+ \lambda^-} \right), \quad t > 0 \quad (18)$$

where $I_\eta(\cdot)$ is the modified Bessel function of parameter η (cf. [2]). The mean and variance of the ISI distribution are (cf. [135]):

$$E(T) = \frac{S}{\delta(\lambda^+ - \lambda^-)}; \quad Var(T) = \frac{S(\lambda^+ + \lambda^-)}{\delta(\lambda^+ - \lambda^-)^3}. \quad (19)$$

When $\delta \rightarrow 0$, assuming $\lambda^+ \sim \lambda^- \sim \frac{1}{2\delta^2}$, this model converges to the Wiener process with $\mu = 0$.

3.4 Stein's model

In 1965 Stein (cf. [132]) formulated the first LIF model, i.e. an IF model with the leakage feature, by introducing the spontaneous membrane decay in the absence of PSP's in the RRW model. The process X is solution of the SDE

$$dX_t = \left(-\frac{X_t}{\theta} + \rho \right) dt + \delta^+ dN_t^+ + \delta^- dN_t^-; \quad X_{t_0} = x_0. \quad (20)$$

Here $\theta > 0$ is the membrane time constant, ρ is the resting potential, N_t^+ and N_t^- are independent Poisson processes of parameters λ^+ and λ^- respectively and $\delta^+ > 0$, $\delta^- < 0$ are the amplitudes of excitatory and inhibitory PSP's. Generally for this model and for all those descending from it one assumes $\rho = 0$, since the case $\rho \neq 0$ can be obtained by the shift $X \mapsto X - \rho$. Following the IF models structure, the spike times are the first crossing times of the process through the boundary and the membrane potential is instantaneously reset to its resting value after each spike. The infinitesimal moments are:

$$M_1(x) = \lim_{h \rightarrow 0} \frac{E[X_{t+h} - X_t | X_t = x]}{h} = -\frac{x}{\theta} + \rho + \lambda^+ \delta^+ + \lambda^- \delta^- \quad (21)$$

$$M_2(x) = \lim_{h \rightarrow 0} \frac{E[(X_{t+h} - X_t)^2 | X_t = x]}{h} = \lambda^+ (\delta^+)^2 + \lambda^- (\delta^-)^2.$$

The mean trajectory, in the absence of a threshold, is

$$E(X_t | X_0 = x_0) = x_0 e^{-t/\theta} + (\lambda^+ \delta^+ + \lambda^- \delta^-) \theta (1 - e^{-t/\theta}). \quad (22)$$

The FPT problem for the process (20) is still unsolved and the use of simulation techniques is required for its analysis.

3.5 Ornstein-Uhlenbeck Diffusion Model

The OU process was proposed as a continuous limit of the Stein model to facilitate the solution of the FPT problem. The rationale for this limit is the huge number of synapses characterizing certain neurons such as the Purkinje cells. The PSP's determine frequent small jumps and limit theorems can be applied to get a diffusion process. The OU process, already known in the Physics literature (cf. [136]), belongs to both classes of Markov and Gaussian stochastic processes.

Different approaches can be followed to obtain the diffusion limit of Stein's model. In [71] the convergence of the measure of a Stein's process to that of the OU one is studied. In [20], [107] it is proved that the continuous limit of the transition pdf for the process (20) converges to a pdf that verifies the Fokker Plank equation for the OU process. Alternatively the OU model can be derived from a differential equation describing the membrane potential dynamics. We sketch in the following these last two approaches.

Due to the time continuity and to the Markov property of Stein's process, the Smolukowsky equation holds for the transition pdf:

$$f(x, t + \Delta t | x_0, t_0) = \int_{-\infty}^{\infty} f(x, t + \Delta t | z, t) f(z, t | x_0, t_0) dz. \quad (23)$$

In the absence of inputs to the neuron, the process (20), initially in the state z at time t , decays exponentially to the zero resting potential, reaching

at time $t + \Delta t$ the value $x_1 = ze^{-\Delta t/\theta}$. In the case of an excitatory or an inhibitory input at time $u \in (t, t + \Delta t)$ the potential becomes $x_2(u) = ze^{-\Delta t/\theta} + \delta^+ e^{-(t+\Delta t-u)/\theta}$ or $x_3(u) = ze^{-\Delta t/\theta} + \delta^- e^{-(t+\Delta t-u)/\theta}$, respectively. Setting $x_i = \frac{1}{\Delta t} \int_t^{t+\Delta t} x_i(u) du$, $i = 2, 3$ the l.h.s. of (23) becomes:

$$f(x, t + \Delta t | z, t) = [1 - (\lambda^+ + \lambda^-) \Delta t] \delta(x - x_1) + \lambda^+ \Delta t \delta(x - x_2) + \lambda^- \Delta t \delta(x - x_3) + o(\Delta t). \quad (24)$$

Hence (23) becomes:

$$f(x, t + \Delta t | x_0, t_0) = e^{\Delta t/\theta} \left\{ [1 - (\lambda^+ + \lambda^-) \Delta t] f(xe^{\Delta t/\theta}, t | x_0, t_0) + \lambda^+ \Delta t f\left(xe^{\Delta t/\theta} - \frac{\delta^+ \theta}{\Delta t} (e^{\Delta t/\theta} - 1), t | x_0, t_0\right) + \lambda^- \Delta t f\left(xe^{\frac{\Delta}{\theta}} - \frac{\delta^- \theta}{\Delta t} (e^{\frac{\Delta}{\theta}} - 1), t | x_0, t_0\right) \right\} + o(\Delta t). \quad (25)$$

Approximating $e^{\Delta t/\theta} \approx \frac{\Delta t}{\theta} + 1$, dividing by Δt , when $\Delta t \rightarrow 0$, (26) becomes

$$\frac{\partial f(x, t | x_0, t_0)}{\partial t} = \frac{\partial}{\partial x} \left(\frac{x}{\theta} f(x, t | x_0, t_0) \right) + \lambda^+ [f(x - \delta^+, t | x_0, t_0) - f(x, t | x_0, t_0)] + \lambda^- [f(x - \delta^-, t | x_0, t_0) - f(x, t | x_0, t_0)]. \quad (26)$$

Developing the terms in square brackets as Taylor series around x

$$\frac{\partial f(x, t | x_0, t_0)}{\partial t} = -\frac{\partial}{\partial x} \left[-\left(\frac{x}{\theta} + \lambda^+ \delta^+ + \lambda^- \delta^- \right) f(x, t | x_0, t_0) \right] + \sum_{n=2}^{\infty} \frac{(-1)^n}{n!} \frac{\partial^n}{\partial x^n} \{ [(\delta^+)^n \lambda^+ + (\delta^-)^n \lambda^-] f(x, t | x_0, t_0) \}. \quad (27)$$

Assuming $\delta^+ = -\delta^- = \delta$, $\lambda^+ \sim \frac{A^+}{\delta} + \frac{\sigma^2}{2\delta^2}$, $\lambda^- \sim \frac{A^-}{\delta} + \frac{\sigma^2}{2\delta^2}$, with σ, A^+, A^- positive constants, for $\delta \rightarrow 0$ we get:

$$\frac{\partial f(x, t | x_0, t_0)}{\partial t} = \frac{\partial}{\partial x} \left[\left(-\frac{x}{\theta} + \mu \right) f(x, t | x_0, t_0) \right] + \frac{\sigma^2}{2} \frac{\partial^2 f(x, t | x_0, t_0)}{\partial x^2}, \quad (28)$$

i.e. the Fokker Plank equation for an OU process with $\mu = A^+ - A^-$. Its solution with an initial delta condition (6) is the transition pdf

$$f_{OU}(x, t | x_0, t_0) \equiv \frac{\partial P(X_t < x | X_{t_0} = x_0)}{\partial x} = \frac{1}{\sigma \sqrt{\pi \theta \left(1 - e^{-\frac{2(t-t_0)}{\theta}}\right)}} \times \exp \left\{ -\frac{\left[x - x_0 e^{-\frac{(t-t_0)}{\theta}} - \mu \theta \left(1 - e^{-\frac{(t-t_0)}{\theta}}\right) \right]^2}{\sigma^2 \theta \left(1 - e^{-\frac{2(t-t_0)}{\theta}}\right)} \right\}. \quad (29)$$

The diffusion interval coincides with the real line and the mean and variance of the OU process X_t with $X_{t_0} = x_0$ are:

$$E(X_t | x_0) = \mu \theta \left(1 - e^{-t/\theta}\right) + x_0 e^{-t/\theta}; \quad Var(X_t | x_0) = \frac{\sigma^2 \theta}{2} \left(1 - e^{-2t/\theta}\right). \quad (30)$$

Properties of the models, as well as the range of validity of some approximate formulae for the FPT problem, depend upon the value of the asymptotic mean depolarization of the process X . Hence in various instances we distinguish between two distinct firing regimes, subthreshold if $E(X_\infty) < S$ and suprathreshold in the opposite case.

Model of LIF type can be interpreted in the frame of threshold detectors theory. The presence of a feeble noise helps the detection of the signal, a characteristic of any threshold detector. In Fig. 1 we plot the mean value of an OU process (30a) together with $E(X_t) - 3Var(X_t)$ and $E(X_t) + 3Var(X_t)$, making use of (30b). The two panels correspond to examples in the subthreshold regime (Panel A) and in the suprathreshold regime (Panel B). The intrinsic random variability determines crossings even in the subthreshold regime.

The OU model can also be obtained from the differential equation for the time evolution of the subthreshold membrane potential in the presence of spontaneous decay of parameter θ and net input μ :

$$\frac{dX_t}{dt} = -\frac{X_t}{\theta} + \mu; \quad X_0 = x_0. \quad (31)$$

Adding a noise term of intensity σ to account for the random PSP's, one gets:

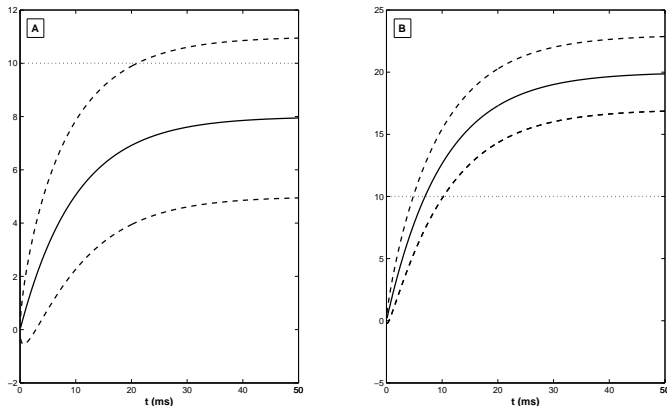


Fig. 1 Mean value (*middle line*) and curves $E(X_t) - 3\text{Var}(X_t)$ (*lower line*) and $E(X_t) + 3\text{Var}(X_t)$ (*upper line*) for an OU process with parameters $\mu = 0.8 \text{ mV ms}^{-1}$, $\sigma^2 = 0.2 \text{ mV}^2 \text{ ms}^{-1}$ and $\theta = 10 \text{ ms}$.

$$dX_t = \left(-\frac{X_t}{\theta} + \mu \right) dt + \sigma dW_t; \quad X_0 = x_0. \quad (32)$$

This is the SDE of an OU process (cf. **SUSANNE**). The analytical expression for the FPT pdf of the OU process is still an open problem. In [5] three alternative representations of the distribution of T are introduced. The first one involves an eigenvalue expansion in terms of zeros of the parabolic cylinder functions while the second is an integral representation involving special functions. We report here the third one that writes the FPT pdf of an OU process with $\mu = 0$ through the boundary S in terms of a three-dimensional Bessel bridge:

$$g(t) = e^{-(S^2 - x_0^2 - t)/2\theta} g_W(t) E_{Bb} \left[\exp \left(-\frac{1}{2\theta^2} \int_0^t (r_s - S)^2 ds \right) \right]. \quad (33)$$

Here $g_W(t)$ is the FPT pdf through the boundary S for the standard Wiener process, r_s is the three-dimensional Bessel bridge over the interval $[0, t]$ between $r_0 = 0$ and $r_t = S - x_0$. This process is solution of:

$$dr_s = \left(\frac{y - r_s}{t - s} + \frac{1}{r_s} \right) ds + dW_s, \quad r_0 = x, \quad s < t. \quad (34)$$

In (33) E_{Bb} indicates the expectation with respect to the Bessel bridge law. In [138] formula (33) is used to approximate the FPT pdf with Monte Carlo techniques.

An explicit expression for the FPT density of continuous Gaussian processes to a general boundary is obtained under mild conditions in [37], while an expression for the FPT of the Wiener process to a curved boundary is expanded as a series of multiple integrals in [38].

Existing available closed form expression include the case of a hyperbolic boundary (cf. [14])

$$S(t) = \mu\theta + Ae^{-\frac{t}{\theta}} + Be^{\frac{t}{\theta}}, \quad (35)$$

with A and B arbitrary constants (cf. [101]). Furthermore specific boundaries can be obtained through the space time transformations described in Section 4.1.2 applied to closed form solutions for the case of the Wiener process. The Laplace transform of the FPT pdf in the case of a constant boundary S is (cf. [102]) :

$$E(e^{-\lambda T}) = \exp\left\{\frac{(x_0 - \mu\theta)^2 - (S - \mu\theta)^2}{2\sigma^2\theta}\right\} \frac{D_{-\lambda\theta}\left[\sqrt{\frac{2}{\sigma^2\theta}}(\mu\theta - x_0)\right]}{D_{-\lambda\theta}\left[\sqrt{\frac{2}{\sigma^2\theta}}(\mu\theta - S)\right]}, \quad (36)$$

where $D_\nu(\cdot)$ is the Parabolic Cylinder Function (cf. [2]) of parameter ν . No analytical inversion formula is available for eq. (36). Reliable and efficient procedures, discussed in Sect. 4, can be applied to obtain the FPT pdf either numerically or by means of simulations for constant or time dependent boundaries.

The FPT mean has been determined as derivative of (36), computed in $\lambda = 0$ (cf. [102]):

$$E(T) = \theta \left\{ \frac{1}{2} \left(\sum_{n=1}^{\infty} \frac{x_S^{2n}}{n(2n-1)!!} - \sum_{n=1}^{\infty} \frac{x_1^{2n}}{n(2n-1)!!} \right) + \sqrt{\pi/2} \left[x_1 \phi\left(\frac{1}{2}, \frac{3}{2}; \frac{x_1^2}{2}\right) - x_S \phi\left(\frac{1}{2}, \frac{3}{2}; \frac{x_S^2}{2}\right) \right] \right\} \quad (37)$$

where $x_1 = (\mu\theta - x_0)\sqrt{2/(\sigma^2\theta)}$, $x_S = (\mu\theta - S)\sqrt{2/(\sigma^2\theta)}$ and $\phi(a, c; z)$ is the Kummer function (cf. [2]). Alternatively the mean is expressed through the Siegert formula (cf. [130]):

$$E(T) = \sqrt{\frac{\pi\theta}{\sigma^2}} \int_{-\mu\theta}^{S-\mu\theta} \left\{ 1 + \operatorname{Erf}\left(\frac{z}{\sigma\sqrt{\theta}}\right) \right\} \exp\left(\frac{z^2}{\sigma^2\theta}\right) dz, \quad (38)$$

where $\operatorname{Erf}(\cdot)$ denotes the error function (cf. [2]).

Use of (37) or (38) depends on the value of the parameters since the two formulae present numerical difficulties for different ranges. Approximate formulae (cf. [84]) hold for specific ranges. If $\mu\theta > S$ and $\sigma \rightarrow 0$, i.e. in the quasi-deterministic case, the mean FPT can be approximated by equating the expression of $E(X_t|x_0)$ with S to obtain (cf. [81]):

$$E(T) \approx -\theta \ln \left(\frac{S - \mu\theta}{x_0 - \mu\theta} \right). \quad (39)$$

Note that (39) disregards the effect of the noise on the crossings. If $x_0 \ll S$, or equivalently if σ is sufficiently small and μ is negative so that the crossing is rare event, the approximation

$$E(T) \approx \frac{\sigma\sqrt{\pi\theta^3}}{S - \mu\theta} \exp\left(\frac{(S - \mu\theta)^2}{\sigma^2\theta}\right) \quad (40)$$

holds (cf. [47]). A linear approximation for the firing rate $f = 1/E(T)$, obtained using (37), is (cf. [84]):

$$f(\mu) = \frac{1}{\pi\theta S} \left(\sigma\sqrt{\pi\theta} + 2\theta\mu - S \right). \quad (41)$$

This approximation holds when $(\mu\sqrt{\theta})/\sigma$ and $(\mu\sqrt{\theta} - S\theta)/\sigma$ are small enough.

When neither (37) nor (38) are suitable for computations and $\mu\tau \gg S$ but σ is not small enough to apply approximation (39) an "ad hoc" procedure to evaluate the mean FPT is possible. One establishes at first the time t_1 at which $E(X_t) + 2\sqrt{\operatorname{Var}(X_t)}$ crosses the threshold S , i.e. when most trajectories are still below the threshold. For $t > t_1$ the process is then approximated by means of the Wiener process with drift μ and initial value $E(X_{t_1})$.

The second moment of the FPT for the OU process is (cf. [92]):

$$\begin{aligned}
E(T^2) &= 2\theta E(T) \left[\sqrt{\pi} \varphi_1\left(\frac{x_s}{\sqrt{2}}\right) + \psi_1\left(\frac{x_s}{\sqrt{2}}\right) \right] \\
&+ 2\theta^2 \left\{ \sqrt{\pi} \ln 2 \left[\varphi_1\left(\frac{x_s}{\sqrt{2}}\right) - \varphi_1\left(\frac{x_1}{\sqrt{2}}\right) \right] \right. \\
&\quad \left. - \sqrt{\pi} \left[\varphi_2\left(\frac{x_s}{\sqrt{2}}\right) + \varphi_2\left(\frac{x_1}{\sqrt{2}}\right) \right] - \psi_2\left(\frac{x_s}{\sqrt{2}}\right) + \psi_2\left(\frac{x_1}{\sqrt{2}}\right) \right\}
\end{aligned} \tag{42}$$

where x_1 , x_S are defined as in (37) and

$$\begin{aligned}
\varphi_1(z) &= \int_0^z e^{t^2} dt = \sum_{k=0}^{\infty} \frac{z^{2k+1}}{k!(2k+1)}; \\
\varphi_2(z) &= \sum_{n=0}^{\infty} \frac{z^{2n+3}}{(n+1)!(2n+3)} \sum_{k=0}^n \frac{1}{2k+1} \\
\psi_1(z) &= 2 \int_0^z e^{u^2} \int_0^u e^{-v^2} dv du = \sum_{k=0}^{\infty} \frac{2kz^{2k+2}}{(2k+1)!(k+1)}; \\
\psi_2(z) &= \sum_{n=0}^{\infty} \frac{2^n z^{2n+4}}{(2n+3)!!(n+2)} \sum_{k=0}^n \frac{1}{k+1}.
\end{aligned} \tag{43}$$

In [22] the mean, variance and skewness of the FPT for the OU process are tabulated for neurobiologically compatible choices of the parameters.

Asymptotic results for the FPT of the OU process are presented in Section 4.1.3.

3.6 Reversal Potential Models

The diffusion interval of the OU process is the real line but large negative values of the membrane potential are unrealistic. Hence other models introduce a saturation effect on the membrane sensibility. When the value of the membrane potential is close to the reversal potential V_I the incoming inputs produce a reduced effect (cf. [78], [44]). A diffusion model with reversal potentials is proposed in [44] as a diffusion limit on a birth and death process. A similar diffusion limit is obtained in [78] from a variant of Stein's model (20) where an inhibitory reversal potential V_I is introduced:

$$dY_t = -\frac{1}{\theta}Y_t dt + \delta^+ dN_t^+ + \left[\varepsilon(Y_t - V_I) + \xi\sqrt{Y_t - V_I} \right] dN_t^-; Y_0 = y_0. \quad (44)$$

Here N_t^+ , N_t^- , δ^+ and θ are the same as in (20), $\varepsilon \in (-1, 0)$, $V_I < x_0$ are two constants and ξ is a suitably defined random variable. The first two infinitesimal moments (3) of this model are:

$$\begin{aligned} \mu(y) &= -y \left(\frac{1}{\theta} - \varepsilon\lambda^- \right) + \delta^+\lambda^+ - \varepsilon\lambda^-V_I; \\ \sigma^2(y) &= \lambda^+(\delta^+)^2 + \lambda^-\varepsilon^2(y - V_I)^2 + \lambda^-Var(\xi)(y - V_I). \end{aligned} \quad (45)$$

The mean trajectory of the process originated in $Y_0 = y_0$ is

$$E(Y_t | y_0) = x_0 e^{-t(\frac{1}{\theta} - \varepsilon\lambda^-)} + \frac{\lambda^+\delta^+ - \varepsilon\lambda^-V_I}{\frac{1}{\theta} - \varepsilon\lambda^-} \left(1 - e^{-t(\frac{1}{\theta} - \varepsilon\lambda^-)} \right). \quad (46)$$

The diffusion limit of this model (known in the neurobiological literature as the Feller model and in other contexts as the Cox-Ingersol-Ross process) is identified with the solution to the SDE (cf. [78])

$$dY_t = \left(-\frac{Y_t}{\tau} + \mu_2 \right) dt + \sigma_2 \sqrt{Y_t - V_I} dW_t; Y_0 = y_0. \quad (47)$$

Here the constants μ_2 , σ_2 and τ are related with those of model (44) by imposing the equality of the infinitesimal moments. One first sets $\tau = \frac{\theta}{1 - \varepsilon\lambda^- - \theta}$ and $\mu_2 = \lambda^+\delta^+ - \varepsilon\lambda^-V_I = \lambda^+\delta^+ - \lambda^-\Delta_I^-$ where $\Delta_I^- = \varepsilon V_I$, then substitutes the variable ξ in (44) by a suitable sequence of r.v.'s such that in the limit for $n \rightarrow \infty$ one gets $Var(\xi_n) = 0$. This choice allows to obtain the same infinitesimal variance at the resting level for the two processes. Hence one gets

$$\sigma_2^2 = -\frac{\lambda^+(\delta^+)^2 + \lambda^-(\Delta_I^-)^2}{V_I}. \quad (48)$$

Note that, due to the expressions for τ and μ_2 , the parameters τ and μ_2 appearing in the SDE (47) bear a different meaning here with respect to the corresponding parameters θ and μ in the OU model. Furthermore $\tau < \theta$.

The diffusion coefficient of the process (47) becomes negative if $X_t < V_I$, hence the diffusion interval is $I = [V_I, \infty)$. The boundary in V_I is regular or exit, depending upon the values of μ_2 and σ_2 , according with the Feller

classification of boundaries (cf. [72]). To determine the transition probability density of the process (47) a boundary condition should be added. The natural choice, that respects the model features, is the reflecting condition:

$$\lim_{x \rightarrow V_I} \left\{ \mu(x) f(x, t | x_0, t_0) - \frac{\partial}{\partial x} [\sigma^2(x) f(x, t | x_0, t_0)] \right\} = 0. \quad (49)$$

The Feller process is generally known in its standardized form

$$dX_t = \left(-\frac{X_t}{\tau} + \mu_F \right) dt + \sigma_2 \sqrt{X_t} dW_t; \quad X_0 = -V_I, \quad (50)$$

that can be easily obtained from (47) by performing the space transformation $Y_t \rightarrow Y_t - V_I$ and by setting $\mu_F = \mu_2 - \frac{V_I}{\tau}$. This equation is defined over $I = [0, \infty)$.

A further notation for the parameters of the Feller process, largely employed in the literature, sets:

$$p \equiv -\frac{1}{\tau}; \quad q \equiv \mu_F; \quad r \equiv \frac{\sigma_2^2}{2}. \quad (51)$$

The transition pdf of the Feller process X depends (cf. [72]) upon the nature of the lower boundary in $x = 0$ for the process (50) or in $x = V_I$ for the process (47) and on the selected boundary condition for the solution of its Kolmogorov equation. If we impose a zero-flux condition (49) in the origin, using the notation (51), we obtain the transition pdf (cf. [44]):

$$\begin{aligned} f_{Fe}(x, t | x_0, t_0) &\equiv \frac{\partial P(X_t < x | X_{t_0} = x_0)}{\partial x} = \frac{p \left(\frac{x}{x_0} e^{-p(t-t_0)} \right)^{\frac{q-r}{2r}}}{r(e^{p(t-t_0)} - 1)} \\ &\times \exp \left\{ -\frac{p(x + x_0 e^{p(t-t_0)})}{r(e^{p(t-t_0)} - 1)} \right\} I_{\frac{q}{r}-1} \left[\frac{2p\sqrt{xx_0 e^{p(t-t_0)}}}{r(e^{p(t-t_0)} - 1)} \right]. \end{aligned} \quad (52)$$

Here $I_\eta(z)$ indicates the modified Bessel function of the first kind (cf. [2]) of parameter η .

The mean trajectory of the process (47) originated in $X_0 = x_0$ is

$$E(X_t | x_0) = x_0 e^{-t/\tau} + \mu_2 \tau (1 - e^{-t/\tau}). \quad (53)$$

while its variance is

$$\text{Var}(X_t | x_0) = \tau \sigma_2^2 \left(1 - e^{-\frac{t}{\tau}}\right) \left\{ \frac{\mu_2 \tau - V_I}{2} \left(1 - e^{-\frac{t}{\tau}}\right) + (x_0 - V_I) e^{-\frac{t}{\tau}} \right\}. \quad (54)$$

The FPT pdf of the Feller process cannot be obtained in a closed form but it can be evaluated by employing the methods described in Sect. 4. Furthermore its Laplace transform is (cf.[43]):

$$g_\lambda(S | x_0) = \frac{\Phi\left(\frac{-\lambda}{p}, \frac{q}{r}; -\frac{px_0}{r}\right)}{\Phi\left(\frac{-\lambda}{p}, \frac{q}{r}; -\frac{pS}{r}\right)}. \quad (55)$$

Here Φ denotes the Kummer function (cf. [2]) and the notation in (51) has been employed. The mean firing time, when $x_0 < S < V_E$, is (cf. [44]):

$$E(T) = \frac{\tau}{\mu_2 \tau - V_I} \left(S - x_0 + \sum_{n=1}^{\infty} \frac{(S - V_I)^{n+1} - (x_0 - V_I)^{n+1}}{(n+1) \prod_{i=1}^n (\mu_2 \tau - V_I + i\tau \sigma_2^2/2)} \right). \quad (56)$$

If $\tau \mu_2 \gg S$ and σ_2 is suitably small, the mean FPT can be approximated with a formula analogous to (39) for the OU process. Indeed it holds:

$$E(T) \approx -\tau \ln \left(\frac{S - \mu_2 \tau}{x_0 - \mu_2 \tau} \right). \quad (57)$$

When the crossing is a rare event, i.e. $x_0 \ll S$ or σ_2 is small, a result analogous to (40) can be derived (cf. [47]):

$$E(T) \approx \frac{S - V_I}{\mu_2 - \frac{S - V_I}{\tau} - \frac{\sigma_2^2}{4}} \Gamma \left(\frac{2(\mu_2 \tau - V_I)}{\sigma_2^2 \tau} \right) \left[\frac{\sigma_2^2 \tau}{2(S - V_I)} \right]^{\frac{2(\mu_2 \tau - V_I)}{\sigma_2^2 \tau}} e^{\left[\frac{2(S - V_I)}{\sigma_2^2 \tau} \right]}. \quad (58)$$

Here Γ denotes the Gamma function (cf. [2]).

The second moment of the FPT has been obtained in [44]:

$$\begin{aligned}
E(T^2) &= \frac{2\tau E(T)}{\mu_2\tau - V_I} \left[S - V_I + \sum_{k=1}^{\infty} \frac{(S - V_I)^{k+1}}{(k+1) \prod_{i=1}^k \left[\mu_2\tau - V_I + \frac{i\tau\sigma_2^2}{2} \right]} \right] \\
&\quad - \sum_{k=1}^{\infty} \frac{2\tau^2 [(S - V_I)^{k+1} - (x_0 - V_I)^{k+1}]}{(\mu_2\tau - V_I)(k+1)} \\
&\quad \times \sum_{j=1}^k \left\{ j \prod_{i=1}^k \left[\mu_2\tau - V_I + \frac{i\tau\sigma_2^2}{2} \right] \right\}^{-1}.
\end{aligned} \tag{59}$$

The expression for the third moment can be found in [107].

A further variant of Stein's model was proposed in [80] with two reversal potentials, an inhibitory (lower) one V_I and an excitatory (upper) one V_E :

$$\begin{aligned}
dX_t &= -\frac{1}{\theta} X_t dt + \delta^+(V_E - X_t) dN_t^+ + [\delta^-(X_t - V_I) \\
&\quad - J\sqrt{(V_E - X_t)(X_t - V_I)}] dN_t^- \\
X_0 &= x_0.
\end{aligned} \tag{60}$$

Here the two independent Poisson processes N^+ and N^- have intensities λ^+ and λ^- , respectively, $-1 < \delta^- < 0 < \delta^+ < 1$, J is a r.v. defined over the interval $(-1 - \delta^-, -\delta^-)$ such that $E(J) = 0$. For a sequence of models (60) indexed by n one can assume that $\delta_n^+, \delta_n^- \rightarrow 0_-, \lambda_n^+, \lambda_n^- \rightarrow \infty$ in such a way that $\delta_n^+ \lambda_n^+ \rightarrow \mu \geq 0$, $\delta_n^- \lambda_n^- \rightarrow \nu \leq 0$. Simultaneously $E(J_n^2) \rightarrow 0_+$ in such a way that $\lambda_n^- E(J_n^2) \rightarrow \sigma_3^2 > 0$. This allows to obtain the diffusion approximation

$$dX_t = \left(-\frac{X_t}{\tau_3} + \mu_3 \right) dt + \sigma_3 \sqrt{(X_t - V_I)(V_E - X_t)} dW_t; \quad X_0 = x_0 \tag{61}$$

where the new constants τ_3 and $\mu_3 = \mu V_E - \nu V_I$ have been introduced.

The diffusion interval of this process is $[V_I, V_E]$ and its transition pdf is solution of the Fokker-Planck equation with initial delta condition and with reflecting conditions of the type (49) on both boundaries V_I and V_E .

The first two moments of the membrane potential (cf. [80]) are:

$$E(X_t | x_0) = x_0 e^{-t/\tau_3} + \mu_3 \tau_3 (1 - e^{-t/\tau_3}) \quad (62)$$

$$E(X_t^2 | x_0) = (V_E - V_I)^2 \left\{ \frac{\beta (2\beta + \sigma_3^2)}{\alpha (2\alpha + \sigma_3^2)} + e^{-\alpha t} \frac{(\beta - \alpha) (2\beta + \sigma_3^2)}{\alpha (\alpha + \sigma_3^2)} \right. \\ \left. + e^{-\alpha t - \sigma_3^2 t} \frac{(\beta - \alpha) (2\beta - 2\alpha + \sigma_3^2)}{(2\alpha + \sigma_3^2) (\alpha + \sigma_3^2)} - e^{-\alpha t} \left[1 - \frac{x_0 - V_I}{V_E - V_I} \right] \right. \\ \left. \left(\frac{2\beta + \sigma_3^2}{\alpha + \sigma_3^2} + e^{-\alpha t - \sigma_3^2 t} \frac{(2\alpha - 2\beta + \sigma_3^2)}{\alpha + \sigma_3^2} \right) + e^{-2\alpha t - \sigma_3^2 t} \left[1 - \frac{x_0 - V_I}{V_E - V_I} \right]^2 \right\}. \quad (63)$$

Here $\alpha = 1/\tau_3$ and $\beta = (-\alpha V_I + \mu_3) / (V_E - V_I)$ and a typo in [80] is corrected. Use of (62) and (63) allows the computation of $Var(X_t | x_0)$.

The mean firing time through a boundary $S < V_E$ is:

$$E(T) = \frac{S - x_0}{\beta (V_E - V_I)} \quad (64) \\ + \sum_{n=0}^{\infty} \frac{\Gamma(2\beta/\sigma_3^2 + 1) \Gamma(2\alpha/\sigma_3^2 + 1) (S - V_I)^{n+2} - (x_0 - V_I)^{n+2}}{\Gamma(2\beta/\sigma_3^2 + n + 2) \Gamma(2\alpha/\sigma_3^2) \beta (n + 2) (V_E - V_I)^{n+2}}.$$

If the boundary crossing is a rare event, a result analogous to (40) and (58) holds ([80]):

$$E(T) \approx \frac{S - x_0}{\beta (V_E - V_I)} \left(1 + \frac{\alpha (S + x_0 - 2V_I)}{(2\beta + \sigma_3^2) (V_E - V_I)} \right) \quad (65)$$

When $\mu_3 \tau_3 > S$, one gets a result analogous to (39) and (57):

$$E(T) \approx -\tau_3 \ln \left(\frac{S - \tau_3 \mu_3}{x_0 - \tau_3 \mu_3} \right). \quad (66)$$

3.7 Comparison between different LIF models

The mathematical complexity of the FPT problem increases with the attempts to make the models more realistic. However it is desirable to avoid the use of complex models when they do not add any improvement with respect to the simpler ones.

In Fig. 2 we compare sample paths from the OU, the Feller process and the process with double reversal potential, simulated using Euler algorithm (cf. **SUSANNE**) on the same leading Wiener process trajectory. Furthermore

we consider $\theta = \tau = 10 \text{ ms}$ and we choose the same level of variability at the resting level for all models. Hence $\sigma_2^2 |V_I| = \sigma^2$ and $\sigma_3^2 V_E |V_I| = \sigma^2$. Since the three processes do not show relevant discrepancies, this analysis suggests to prefer the first two models due to their better computational tractability.

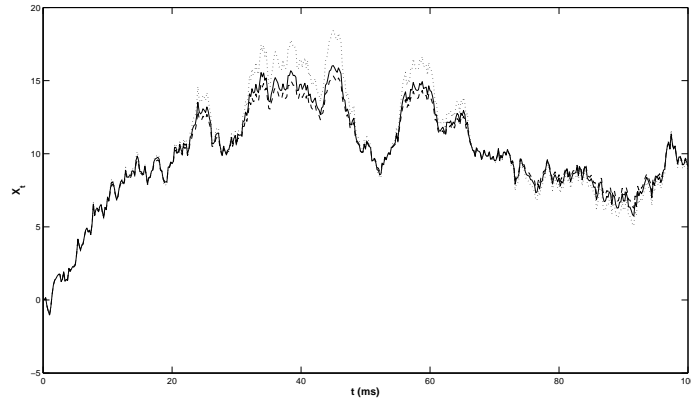


Fig. 2 Sample paths of the OU (*dashed line*), the Feller (*dotted line*) and the double reversal potential (*continuous line*) models employing the same leading Wiener process realization. Here $\mu = \mu_2 = \mu_3 = 1 \text{ mVms}^{-1}$, $\sigma^2 = 0.9 \text{ mV}^2\text{ms}^{-1}$, $V_I = -10 \text{ mV}$, $V_E = 30 \text{ mV}$.

When one wish to compare the FPT pdf's one gets different results according with the selected criterium for the parameters values. In [81] the OU and of the Feller ISIs, computed through (??), are compared, according with three different criteria:

- to get the same values for their corresponding discrete versions:

$$\mu = \mu_2; \quad \sigma^2 = -\sigma_2^2 V_I,$$

θ and τ chosen accordingly (cf. Fig. 3A);

- to get the same mean trajectory for both models (Fig. 3B):

$$\begin{aligned} \theta &= \tau; \quad \mu = \mu_2 \\ \sigma &= \sigma_2 \sqrt{-V_I}; \end{aligned}$$

- to get almost equal FPT densities. For this aim, one fixes the parameters for one model and determines a set of parameters, reproducing a similar ISI distribution, for the other one (cf. Fig. 3 C). To guess possible set of parameters for the second process we impose the equality of the mean and the variance of their FPT's.

The last case illustrates the evenience where a histogram of experimentally obtained ISI's can be fitted by either of the two model distributions.

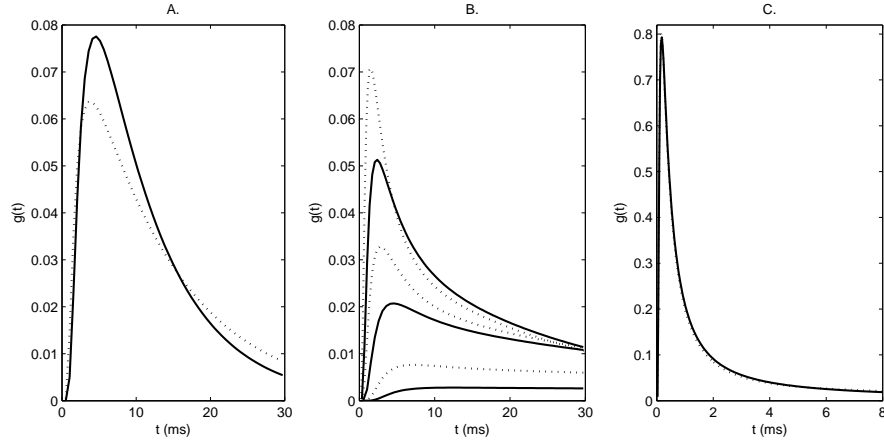


Fig. 3 Comparisons between the OU (*continuous line*) and the Feller (*dashed lines*) models. **Panel A:** $V_I = -10$ mV, $S = 10$ mV, $\theta = 6.2$ ms; parameters controlling the PSP sizes and the intensities of the input processes: $a_e = -i_I = 2$ mV, $\epsilon = -0.2$, $\lambda = 8/\theta \cong 1.290$ ms^{-1} , $\omega = 4/\theta \cong 0.641$ ms^{-1} . **Panel B:** $x_0 = 0$ mV, $V_I = -10$ mV, $S = 10$ mV, $\theta = \tau = 6.2$ mV, $\sigma^2 = 4, 9$ and 16 mV^2ms^{-1} (from bottom to top), $\mu = \mu_F = 0$ $mVms^{-1}$. **Panel C:** Feller model $y_0 = 0$ mV, $S = 5$ mV, $V_I = -10$ mV, $\tau = 6.2$ ms, $\mu_2 = 0$ $mVms^{-1}$, $\sigma_2^2 = 4$ $mVms^{-1}$; OU model $x_0 = 0$ mV, $S = 5$ mV, $\theta = 6.2$ ms, $\mu = -0.799$ $mVms^{-1}$, $\sigma^2 = 48.03$ mV^2ms^{-1} .

The use of the more complex Feller model seems preferable when one has data of the membrane potential between consecutive spikes ([81]). When only the ISI distribution is available, both models fit the data. In ([119]) qualitative comparisons between the OU and the Feller processes, obtained through the stochastic ordering techniques (cf. [123]) in Subsubsection. 4.1.5, are presented. In ([118]) the same techniques are used for a sensitivity analysis on

the parameters of the FPT pdf. Stochastic ordering properties of the FPT's are used in [30] to select the model.

Membrane potential data analyzed in [67] show that the same neuron, under different experimental conditions, can be described either by the OU model, by the Feller model or by an alternative model with a quadratic diffusion coefficient.

3.8 Jump diffusion models

In Subsections (3.5) and (3.6), to perform the diffusion limits, it was assumed that all the contributions to the changes in the membrane potential were of the same small amplitude and the frequency was large enough (cf. [20]). However PSP's impinging on the soma can play a different role with respect to the contributions on different areas of the neuron.

LIF models where the subthreshold membrane potential dynamics is described by jump diffusion processes allow to separate inputs according to their strongness. Jump diffusion models can be obtained from a variant of the Stein-type model:

$$\begin{aligned} dX_t &= -\frac{X_t}{\theta}dt + \sum_{j=1}^n \delta_j^+ dN_t^{+,j} + \sum_{k=1}^m \delta_k^- dN_t^{-,k} + \delta^e dN_t^e + \delta^i dN_t^i \\ X_{t_0} &= x_0. \end{aligned} \quad (67)$$

Here N_t^e, N_t^i are independent Poisson processes of parameters λ^e and λ^i and amplitude δ^e and δ^i accounting for the strong contributions. $N_t^{+,j}, N_t^{-,k}$ are independent Poisson processes of parameters λ_j^+ and λ_k^- , independent from N_t^e and N_t^i . If $\delta_j^+, \delta_k^- \rightarrow 0$ and at the same time $\lambda_j^+, \lambda_k^- \rightarrow \infty$ so that $\delta_j^+ \lambda_j^+ + \delta_j^- \lambda_j^- \rightarrow \mu$ and $(\delta_j^+)^2 \lambda_j^+ + (\delta_j^-)^2 \lambda_j^- \rightarrow \sigma^2$, a diffusion approximation can be performed to get a process solution of the SDE:

$$dX_t = \left(-\frac{X_t}{\theta} + \mu \right) dt + \sigma^2 dW_t + \delta^e dN_t^e + \delta^i dN_t^i; \quad X_{t_0} = x_0 \quad (68)$$

where W is independent from N_t^e and N_t^i . The model (68) is a jump diffusion process with an OU underlying diffusion. Other jump diffusion models may

be obtained introducing the reversal potentials. All these models are of LIF type, requiring the superposition of a boundary S to mimic the spike activity. The crossings can occur either for diffusion or for an upward jump when $X \in (S - \delta^e, S)$. Hence the spike time is the time of first entrance (FET) into the strip (S, ∞) . The cases of underlying Wiener with drift and OU process have been considered in ([79], [56], [120], [131]). The exponential distribution for the jump epochs preserves the Markov property of the process (68). In [120] and [124] the case of IG distributed jump epochs is discussed but in this instance the resulting process is no more a Markov one.

To compute the ISI distribution for IG and exponential time distributed jumps one resorts to simulation techniques. Differently from the unimodal behavior of the ISI distribution of diffusion models, jump diffusion ones have a multimodal shape (cf. Fig. 4).

The only analytical results on the FET problem for jump diffusions refer to an underlying Wiener process with constant boundary. Lower bounds are proposed in [31] for the FET density and in [57] for the FET mean and variance, together with exact formulae for the specific case of large jumps, when the jumps are driven by a counting process. An approximate solution to an integral equation for the FET density of a jump diffusion process is discussed in [59] for the Wiener process.

3.9 Boundary shapes

Constant thresholds are typically employed in LIF models for their easier mathematical tractability. However the refractory period following each spike has been modelled by means of threshold shapes (cf. [101], [52]). These boundaries attain very high values after a spike, then decrease under the reference value and finally oscillate around a constant value (cf. Fig. 5, panel A).

In [23] a dynamic threshold obeying to a differential equation is considered for the same aim. A boundary which is a linear combination of two exponentials with different time constants is proposed in [75], to fit experimental data. The use of this boundary, together with the lack of the resetting of the membrane potential after a spike, allows a very good fit of the data. A computational method that can reproduce and predict a variety of spike

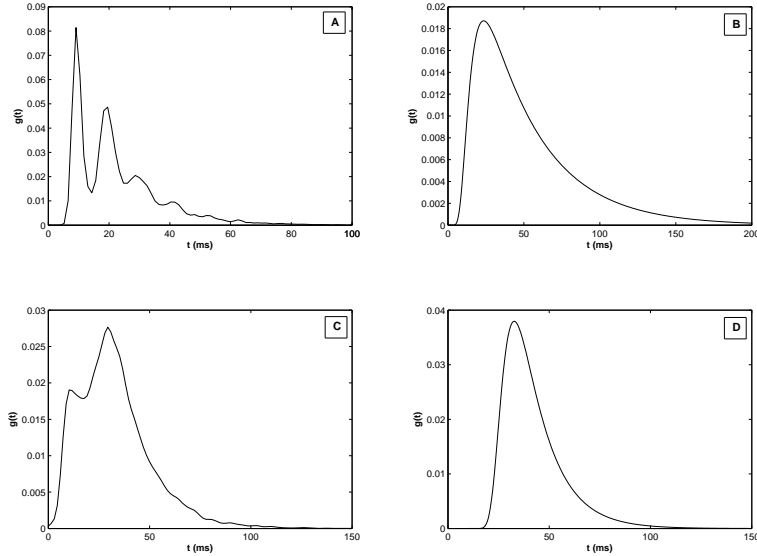


Fig. 4 Examples of ISI distributions for jump-diffusion processes (68); underlying OU diffusion process with different parameters for Panels A and B, C and D. **Panel A:** IG time distributed jumps. **Panel C:** Exponential jump interarrivals. **Panel B, Panel D:** ISI distribution for pure OU diffusion, parameters as in Panels A and C respectively.

responses has been devised in [76] using a multi-timescale adaptive threshold predictor and a nonresetting leaky integrator.

In [24], [25] thresholds with fatigue are proposed to account for experimental data showing a progressive decrease of excitability during high frequency firing. This type of threshold destroys the renewal and Markov character of the process but allows to describe adaptation phenomena through LIF models. The inclusion of time dependent boundaries prevents the use of many mathematical methods described in the next Section, however reliable numerical and simulation techniques can be applied (cf. Sect. 4).

Finally, the study of periodic boundaries or of noisy thresholds ([89]) becomes a useful mathematical method to deal with periodic inputs. Indeed one transforms the original process with time periodic drift and constant boundary into a time homogeneous diffusion process, constrained by a periodic absorbing boundary (cf. [100], [129], [94]). To illustrate this idea let

us consider an OU model with periodic input of frequency ω , phase φ and amplitude A . The SDE (32) for this LIF model is

$$dX_t = \left(-\frac{X_t}{\theta} + \mu + A \sin(\omega t + \varphi) \right) dt + \sigma dW_t; \quad X_0 = x_0 \quad (69)$$

with $x_0 < S$. X is not an OU process, however the change of space variable

$$Y_t = X_t - \frac{A\theta}{\sqrt{1 + (\omega\theta)^2}} \left[\sin(\omega t + \varphi - \xi) - e^{-t/\theta} \sin(\varphi - \xi) \right] \quad (70)$$

with $\xi = \arctan(\omega\theta)$ transforms (69) into the SDE of an OU process with parameters θ , μ and σ , $y_0 = x_0$, and the constant boundary S into

$$S(t) = S - \frac{A\theta}{\sqrt{1 + (\omega\theta)^2}} \left[\sin(\omega t + \varphi - \xi) - e^{-t/\theta} \sin(\varphi - \xi) \right]. \quad (71)$$

The ISI's of the periodically modulated LIF model with constant threshold are distributed as the ISI's of a LIF model with constant input and appropriate time-dependent threshold (cf. Fig. 5).

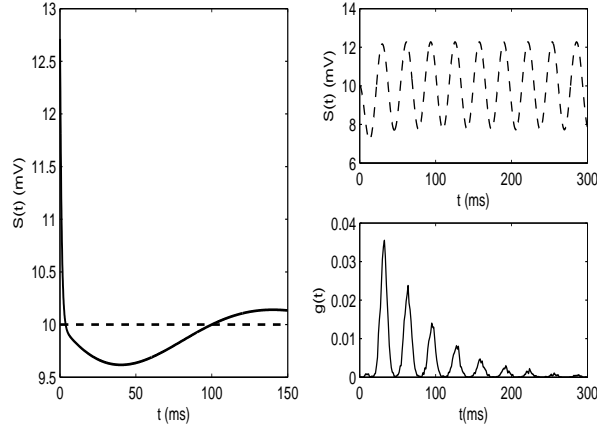


Fig. 5 Panel A: Time dependent threshold $S(t) = 10 + 3e^{-t} - 0.6e^{-\frac{t}{100}} \sin(\frac{\pi t}{100})$. **Panel B:** Threshold of the transformed process (upper) and simulated FPT pdf (lower) for an OU process with additional sinusoidal term in the drift coefficient.

3.10 Further models

New efforts on LIF models are mainly devoted to the study of input-output relationships or to the analysis of small neuronal networks with units described by LIF models (cf. [131]). New variants of LIF models have recently appeared in the literature to catch further features such as plasticity (cf. [42]) or to improve their flexibility and their predictive power (cf. for example [13], [26], [16]). We quote also the LIF compartmental models (cf. [83], [109], [110], [111]) that extend the one dimensional ones by introducing systems of SDE's to describe the dynamics of different components of the neuron such as the dendritic and the soma zone in the case of two compartmental models. These models require the study of the FPT of one component through a boundary to describe the ISI's. Up to now this problem can be handled only through simulations.

3.11 Refractoriness and return process models

An alternative approach to the study of spike trains focus on the number of spikes in a prescribed time interval. This study allows to introduce the refractoriness of the neuron in a quite natural way. To this aim one can associate a return process $\{Z = Z_t, t \geq 0\}$ in the interval (l, S) , $S \in I$, to any regular diffusion process $X = \{X_t : t \geq 0\}$ on $I = (l, r)$ as follows. Starting at $x_0 \in (l, S)$ at time 0, the process Z coincides with X until it attains the level S . At this time it is blocked on the boundary S for a random time and no new crossings can occur during this refractory period. Then Z and X are instantaneously reset at x_0 and the process Z evolves as X until the boundary S is reached again, and so on. We show in Fig. 6 a sample path of this process when the refractory period is constant.

Let F_i and R_i , $i = 0, 1, \dots$, be the r.v.'s describing the time between the i -th reset and the $(i+1)$ -th crossing and the i -th refractory period. For time-homogeneous diffusions, the r.v.'s F_i are iid with pdf $g(S, t | x_0)$. It is also assumed that the r.v.'s R_i , $i = 0, 1, \dots$, are iid with pdf $\varphi(t)$ depending only on the duration of the refractory period.

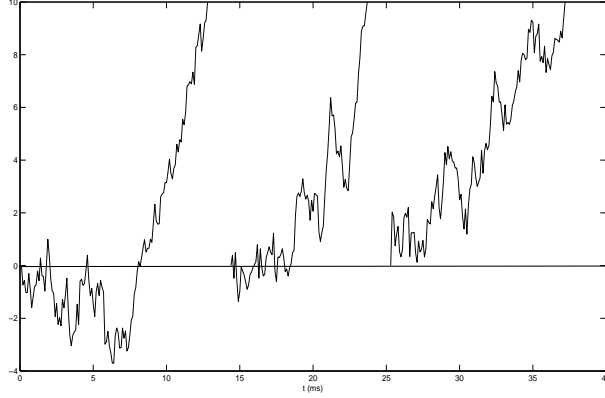


Fig. 6 Sample path of a return process Z with a constant refractory period.

A counting process $M = \{M_t, t \geq 0\}$ can be introduced to describe the number of attainments of the level S by the process Z up to time t . Let

$$q_k(t|x_0) = P\{M_t = k | Z_0 = x_0\}, \quad k = 0, 1, \dots \quad (72)$$

be the probability that k firings occur up to t . Then (cf. [108]):

$$q_0(t|x_0) = 1 - \int_0^t g(S, \tau | x_0) d\tau \quad (73)$$

$$q_k(t|x_0) = [g(S, t | x_0) * \varphi(t)]^{(k)} * \left[1 - \int_0^t g(S, \tau | x_0) d\tau\right] + g(S, t | x_0) \\ * [\varphi(t) * g(S, t | x_0)]^{(k-1)} * \left[1 - \int_0^t \varphi(\tau) d\tau\right] \quad k = 1, 2, \dots \quad (74)$$

where $*$ means convolution and exponent (k) denotes (k) -fold convolution.

Expressions for such probabilities have been obtained in [3] for the Wiener process for exponentially distributed refractory periods. In the general time homogeneous case

$$E\{M_t^r | x_0\} = \sum_{k \geq 1} k^r q_k(t|x_0) \quad r = 1, 2, \dots \quad (75)$$

is the r -th order moment of M . Let I_i , $i = 0, 1, 2, \dots$ be the r.v.'s describing the ISI's and let I_0 be the time of the first firing. One has (cf. [49]):

$$\begin{aligned}
E(I) &= t_1(S|x_0) + E(R); \quad E(I^2) = t_2(S|x_0) + E(R^2) + 2E(R)t_1(S|x_0) \\
E(I^3) &= t_3(S|x_0) + E(R^3) + 3E(R)t_2(S|x_0) + 3E(R^2)t_1(S|x_0)
\end{aligned} \tag{76}$$

where $t_r(S|x_0)$ is the r -th order moment of the FPT. If the first three moments of the refractory period are finite, the following asymptotic expressions for large times hold for the first two moments of M (cf. [49]):

$$E\{M_t|x_0\} \cong \frac{1}{E(I)}t + \frac{1}{2} \frac{E(I^2)}{E^2(I)} - \frac{t_1(S|x_0)}{E(I)}; \tag{77}$$

$$\begin{aligned}
E\{[M_t]^2|x_0\} &\cong \frac{1}{E^2(I)}t^2 + \left[\frac{2E(I^2)}{E^3(I)} - \frac{1}{E(I)} - \frac{2t_1(S|x_0)}{E^2(I)} \right] t \\
&+ \frac{3}{2} \frac{E^2(I^2)}{E^4(I)} - \frac{2}{3} \frac{E(I^3)}{E^3(I)} - \frac{1}{2} \frac{E(I^2)}{E^2(I)} + \frac{t_1(S|x_0)}{E(I)} \\
&+ \frac{t_2(S|x_0)}{E^2(I)} - \frac{2E(I^2)}{E^3(I)}t_1(S|x_0).
\end{aligned} \tag{78}$$

In [48] and [106] the case of absence of refractory period and that of a random distribution for the return value are discussed for the Wiener, OU and Feller processes. Alternatively [17] proposes to model refractoriness through return processes characterized by an elastic boundary as firing threshold.

4 Mathematical methods for First Passage time problem and their application to the study of neuronal models

We update here previous reviews ([1], [105] and [107]) on the methods available up to now to deal with the FPT problem for stochastic LIF models.

In the case of diffusion processes, closed form expressions for the transition pdf's are determined as solutions of the Kolmogorov or the Fokker-Plank equations of Subsections 3.2, 3.5 and 3.6. The Fourier transform is the typical method to get these solutions.

Closed form solutions for the FPT pdf refers generally to specific time dependent boundaries. The constant boundary case is known for the Wiener process (cf. (11)) or for the OU one if $S = 0, \mu = 0$ and $x_0 \neq 0$. The FPT

pdf has been determined for the hyperbolic shape boundary (35) for the OU process (cf. [101]) or for the Feller process (cf. [115]) in the case of boundaries corresponding to symmetries for these processes. Use of the reflection principle allows to determine the FPT pdf through Daniels' boundary ([28], [29], [88]) while a particular FPT pdf is found through a symmetry based constructive approach in [45]. The theory of group transformations is used in [115] and [54] to determine the transition pdf's of a Feller process between the origin and a hyperbolic-type boundary and of an OU process between a lower reflecting and an upper absorbing constant boundary, but is of no interest for neuronal application and hence we omit the description of this method.

In Subsect. 4.1 we review the commonly used analytical techniques for FPT problems: integral equations (4.1.1), change of variables or of measure (4.1.2), asymptotic studies (4.1.3), computation of FPT moments (4.1.4), stochastic ordering (4.1.5). In Subsubsect. 4.1.6 we present the available methods for jump diffusion processes. In Subsect.(4.2) we introduce the direct (4.2.1) and inverse (4.2.2) FPT problem. Finally in (4.3) we sketch specific simulation techniques for FPT's and the numerical tools for their solution.

4.1 Analytical methods

4.1.1 Integral equations

In 1943 Fortet ([40]) proved, under mild conditions for the boundary $S(t)$, that the Volterra integral equation of the first kind:

$$f(x, t | x_0) = \int_0^t g(S(\tau), \tau | x_0) f(x, t | S(\tau), \tau) d\tau, \quad (79)$$

holding for $x > S(t)$, holds also for $x = S(t)$.

When the boundary is constant and the process is time homogeneous, eq. (79) is of convolution type and the Laplace transform method can be applied. Denoting as $f_\lambda(S | x_0)$ and $g_\lambda(S | x_0)$ the Laplace transforms of $f(S, t | x_0)$ and of $g(S, t | x_0)$, for $x > S > x_0$ one gets:

$$g_\lambda(S|x_0) = \frac{f_\lambda(x|x_0)}{f_\lambda(x|S)}. \quad (80)$$

Generally the Laplace transform cannot be analytically inverted due to its complex expression (cf. for example (36)).

Eq. (79) for $x = S(t)$ has a weakly singular kernel for $\tau \rightarrow t$. Indeed, any diffusion behaves as a Wiener process for small times. Hence $f(S(t), t|S(\tau), \tau) \approx \frac{k(t, \tau)}{\sqrt{t-\tau}}$ with $k(t, \tau) \rightarrow 0$ as $\tau \rightarrow t$. This makes numerical methods for their solution unstable. Hence it is convenient to switch to a second type Volterra equation. Integrating (79) between the left side of the diffusion interval l and $S(t)$ and then differentiating with respect to time, one gets a second kind Volterra equation (cf. [104]):

$$g(S(t), t|x_0) = 2j(S(t), t|x_0) - 2 \int_0^t g(S(t), t|x_0) j(S(t), t|S(\tau), \tau) d\tau, \quad (81)$$

Here we have introduced the probability current through z at time u of the diffusion process X whose pdf is solution of (5):

$$j(z, u|w, v) = \mu(z) f(z, u|w, v) - \frac{1}{2} \left\{ \frac{\partial}{\partial y} [\sigma^2(y) f(y, u|w, v)] \right\} \Big|_{y=z}. \quad (82)$$

Eq. 81 has a weakly singular kernel. For the Wiener process, when $\left| \frac{dS(t)}{dt} \right| \leq Ct^{-\alpha}$, with $\alpha < 1/2$, C a constant and $\lim_{t \rightarrow 0} S(t) > W_{t_0} = x_0$, $g(S(t), t|x_0)$ is the only L^2 solution of (81). It can be expressed as (cf. [104])

$$\begin{aligned} g(S(t), t|x_0) &= 2j(S(t), t|x_0) - 4 \int_0^t d\tau j(S(t), t|S(\tau), \tau) j(S(\tau), \tau|x_0) \\ &\quad + \sum_{n=1}^{\infty} 4^n \int_0^t d\tau j_n(S(t), t|S(\tau), \tau) \\ &\quad \times \left\{ 2j(S(\tau), \tau|x_0) - 4 \int_0^\tau d\theta j(S(\tau), \tau|S(\theta), \theta) j(S(\theta), \theta|x_0) \right\} \end{aligned} \quad (83)$$

where

$$j_n(S(t), t|S(\tau), \tau) = \int_\tau^t d\theta j_1(S(\theta), \theta|S(\tau), \tau) j_{n-1}(S(t), t|S(\theta), \theta) \quad (84)$$

for $n = 2, 3, \dots$ and

$$j_1(S(t), t | S(\tau), \tau) = \int_{\tau}^t d\theta j(S(\theta), \theta | S(\tau), \tau) j(S(t), t | S(\theta), \theta). \quad (85)$$

A third integral equation was proposed in [14]:

$$g(S(t), t | x_0) = -2\psi(S(t), t | x_0) + 2 \int_0^t g(S(t), t | x_0) \psi(S(t), t | S(\tau), \tau) d\tau \quad (86)$$

where

$$\psi(S(t), t | x, \tau) = \frac{d}{dt} \{F(S(t), t | x, \tau)\} + k(t) f(S(t), t | x, \tau). \quad (87)$$

Here $F(S(t), t | x, \tau) = \int_t^{S(t)} f(y, t | x, \tau) dy$ and $k(t)$ is an arbitrary continuous function. A suitable choice for $k(t)$ allows to make the kernel of (86) regular and hence eq. (86) becomes optimal for numerical integration. For example the expressions (87) for the OU and the Feller processes, respectively, that make the kernel of (86) regular are (cf. [14])

$$\begin{aligned} \psi_{OU}(S(t), t | x, \tau) &= \left[\frac{S'(t) + S(t)/\theta - \mu}{2} + \frac{e^{\frac{t-\tau}{\theta}}}{\theta(1 - e^{\frac{2(t-\tau)}{\theta}})} \right. \\ &\quad \left. \times \left([S(t) - \mu\theta]e^{\frac{t-\tau}{\theta}} - x + \mu\theta \right) \right] f(S(t), t | x, \tau) \end{aligned} \quad (88)$$

and

$$\begin{aligned} \psi_{Fel}(S(t), t | x, \tau) &= \frac{p \left[\frac{S(t) - p(t-\tau)}{x} \right]^{\frac{(q-r)}{2r}}}{r[e^{p(t-\tau)} - 1]} \exp \left\{ -\frac{p[S(t) + xe^{p(t-\tau)}]}{r[e^{p(t-\tau)} - 1]} \right\} \\ &\quad \times \left\{ \left[S'(t) - \frac{pS(t)e^{p(t-\tau)}}{e^{p(t-\tau)} - 1} + \frac{1}{2} [pS(t) + q - \frac{r}{2} - S'(t)] \right] \right. \\ &\quad \times I_{q/r-1} \left[\frac{2p\sqrt{S(t)xe^{p(t-\tau)}}}{r[e^{p(t-\tau)} - 1]} \right] \\ &\quad \left. + \frac{p\sqrt{S(t)xe^{p(t-\tau)}}}{e^{p(t-\tau)} - 1} I_{q/r} \left[\frac{2p\sqrt{S(t)xe^{p(t-\tau)}}}{r[e^{p(t-\tau)} - 1]} \right] \right\}. \end{aligned} \quad (89)$$

Other choices for $k(t)$ make the integral on the r.h.s. of (86) vanish for boundaries with particular symmetry properties, such as (35) for the OU process. Infinite sum expansions, bounds and approximations for $g(S(t), t | x_0)$ can be obtained from (86) (cf. [117]).

Expressions that regularize the kernel of eq. (86) can be found also in other specific cases.

4.1.2 Change of variables or change of measures

The transition pdf and the FPT pdf of an assigned processes can be obtained through changes of variables and/or changes of measure.

Let $Y = \{Y_t, t \geq 0\}$ be a diffusion process with $I \subseteq \mathfrak{R}$, characterized by drift $\mu(y, t)$ and diffusion coefficient $\sigma(y, t)$. One may wish to transform this process into a Wiener process through suitable space-time transformations, when this transformation exists. In [100] it is shown that a transformation, conserving the probability mass, mapping the Kolmogorov equation of the process Y into the analogous equation for the Wiener process

$$\frac{\partial f'}{\partial \tau'} + \frac{\partial^2 f'}{\partial y'^2} = 0, \quad (90)$$

with initial delta condition is of the form

$$\tau' = \phi(\tau); \quad y' = \psi(y, \tau); \quad f(x, t | y, \tau) dx = f'(x', t' | y', \tau') dx'. \quad (91)$$

This transformation exists if and only if the infinitesimal moments verify

$$\mu(y, \tau) = \frac{\sigma_y'^2(y, \tau)}{2} + \frac{\sigma(y, \tau)}{2} \left\{ c_1(\tau) + \int_z^y dx \frac{c_2(\tau) \sigma^2(x, \tau) + \sigma_\tau'^2(x, \tau)}{[\sigma(x, \tau)]^3} \right\}. \quad (92)$$

Here $z \in I$ is an arbitrary value and $c_1(t)$ and $c_2(t)$ are arbitrary functions of time. If (92) holds the transformation is:

$$\begin{aligned}
y' &= \psi(y, \tau) = \sqrt{k_1} \exp \left[-\frac{1}{2} \int_{\tau_0}^{\tau} duc_2(u) \right] \int_z^y \frac{dx}{\sigma(x, \tau)} \\
&\quad - \frac{\sqrt{k_1}}{2} \int_{\tau_2}^{\tau} duc_1(u) \exp \left[-\frac{1}{2} \int_{\tau_0}^u d\theta c_2(\theta) \right] + k_2 \\
\tau' &= \phi(\tau) = k_1 \int_{\tau_1}^{\tau} du \exp \left[-\int_{\tau_0}^u d\theta c_2(\theta) \right] + k_3 \\
f(x, t | y, \tau) dx &= f'(x', t' | y', \tau') dx' \tag{93}
\end{aligned}$$

where $z \in I$, $\tau_i \in [0, \infty)$ and k_i , $i = 1, 2, 3$ are constants with $k_1 > 0$. For example the transformation

$$\begin{aligned}
y' &= \psi(y, \tau) = \frac{\sqrt{k_1}}{\sigma} e^{\frac{\tau-\tau_0}{\theta}} (y-z) + \frac{\theta\sqrt{k_1}(\frac{z}{\theta} - \mu)}{\sigma} \left[e^{\frac{\tau-\tau_0}{\theta}} - e^{\frac{\tau_2-\tau_0}{\theta}} \right] \\
&\quad + k_2 \\
\tau' &= \phi(\tau) = \frac{k_1\theta}{2} \left[e^{\frac{2(\tau-\tau_0)}{\theta}} - e^{\frac{2(\tau_1-\tau_0)}{\theta}} \right] + k_3 \\
f(x, t | y, \tau) dx &= f'(x', t' | y', \tau') dx' \tag{94}
\end{aligned}$$

changes the OU process into a Wiener process. Here $\tau_1, \tau_2 > 0$ are arbitrary times. The transformation (94) sends the linear boundary $S(t) = a + bt$ for the Wiener process into the U-shaped boundary (35) for the OU process.

The Feller process can be transformed into the Wiener one, conserving the probability mass, only if $\frac{a}{r} = \frac{1}{2}$. In [21] a necessary and sufficient condition analogous to (92) is given to transform a diffusion process Y into a Feller process.

A change between the measures of two processes is considered in [116], [5] and [6]. In [5] the Girsanov theorem (cf. [112]) and the change of measure

$$dP^{OU} = \exp \left[-\frac{1}{2\theta} (W_t^2 - x_0^2 - t) - \frac{1}{2\theta^2} \int_0^t W_s^2 ds \right] dP \tag{95}$$

are applied to the OU process to obtain its FPT pdf through a constant boundary. Here P^{OU} and P denote the distributions of an OU process with $\mu = 0$ and of a standard Wiener process, respectively.

4.1.3 Asymptotic results

Asymptotic results play an important role in the study of the FPT pdf because they hold from relatively small values of the involved variable. Studies on the asymptotic behavior of the FPT pdf belong to two different classes: large values of the boundary and large times. Let us first list asymptotic results in the first class. In ([92]) the asymptotic exponentiality of the FPT for an OU process is proved; this result is extended in [91] to a class of diffusion processes admitting steady-state density

$$W(x) = \lim_{t \rightarrow \infty} f(x, t | x_0) = \frac{c}{\sigma^2(x)} \exp \left(\int^x \frac{2\mu(y)}{\sigma^2(y)} dy \right), \quad (96)$$

where c is a normalization constant. When the boundary S approaches the unattainable level r of the diffusion interval, $\lim_{x \rightarrow r} \sigma^2(x) [W(x)]^2 E(T) = 0$, the following asymptotic result for the FPT pdf $g(t)$ holds:

$$g(t) \approx \frac{1}{E(T)} \exp \left\{ -\frac{t}{E(T)} \right\}. \quad (97)$$

Numerical studies on the OU and on the Feller processes show that this behavior is attained with a negligible error for quite small values of the boundary S (i.e. for $S = 3$ if $\mu = 0$, $\theta = 1$ and $\sigma^2 = 1$ for the OU process). In this asymptotic case the mean FPT, $E(T)$, loses the dependency upon the initial value x_0 . Asymptotic results hold for the same processes in the case of boundaries either asymptotically constant or asymptotically periodic [47]. Periodic boundaries for the OU process are considered also in [114] (see [107] for a review on time dependent boundaries).

Let us now switch to the asymptotic behavior with respect to time. For small times, the FPT can be approximated with the IG distribution. Indeed near the origin any diffusion process can be approximated by a Wiener process. In [47] the asymptotic behaviour, for large t , of the FPT pdf's through some time-varying boundaries is considered. This paper deals with a class of one dimensional diffusion processes with steady-state density. The considered boundaries include periodic boundaries. Sufficient conditions for an asymptotic exponential behavior are given for the cases of asymptotically constant and asymptotically periodic boundaries. Explicit expressions are worked out

for the processes that can be obtained from the OU process by spatial transformations.

The FPT pdf as $t \rightarrow \infty$, for periodic or asymptotically periodic boundaries $S(t)$, under mild conditions (cf. [47]) exhibits damped oscillations with the same period T as the boundary:

$$g(S(t), t|x_0) \approx \alpha(t) \exp \left\{ - \int_0^t \alpha(\tau) d\tau \right\}. \quad (98)$$

Here $\alpha(t)$ is a periodic function of period T :

$$\begin{aligned} \alpha(t) &= -2 \lim_{n \rightarrow \infty} \psi [S(t + nT), t + nT | x_0] \\ &= - \left\{ V'(t) + \mu[V(t)] - \frac{d}{dt} \frac{\sigma^2[V(t)]}{4} \right\} W[V(t)] \end{aligned} \quad (99)$$

and $V(t) = \lim_{n \rightarrow \infty} S(t + nT)$. This behavior arises also for times not too far from the origin. An exponential asymptotic behavior is also proved for large times and constant boundaries in [127].

An asymptotic evaluation of the probability that the Wiener process first crosses a square root boundary is provided in [126]. Denoting as T_c the FPT of the Wiener process trough the boundary $c\sqrt{1+t}$ one has

$$P(T_c > t) \sim_{t \rightarrow \infty} qt^{-p(c)}, \quad 0 < p(c) < \frac{1}{2}. \quad (100)$$

Here $\lim_{c \rightarrow \infty} p(c) = 0$; $\lim_{c \rightarrow 0} p(c) = \frac{1}{2}$ and $2p(c)$ is a real solution between 0 and 1 with respect to λ of the equation:

$$\sum_{n=1}^{\infty} \frac{\sin(\frac{\pi\lambda}{2})\Gamma(1 + \frac{\lambda}{2})(\sqrt{2}c)^n}{\pi n!} \Gamma(\frac{n-\lambda}{2}) = 1. \quad (101)$$

Using the inverse of transformation (94), this result can be applied to get the asymptotic OU process FPT pdf trough a constant boundary for large times.

In [?] truncations of the series expansion of the FPT pdf solution of (86) are used to achieve approximate evaluations. Use of fixed point theorems is made to obtain bounds for the FPT pdf of the OU and the Feller processes. Inequalities are proved to find for which times the FPT pdf can be approxi-

mated, within a preassigned error, by means of an assigned distribution such as the FPT of the Wiener process or the exponential one.

In [93] the asymptotic behavior of the FPT pdf through time-varying boundaries is determined for a class of Gauss-Markov processes.

4.1.4 Moments of the FPT

Analytical formulae for the moments of the FPT are available only for time homogeneous processes with constant boundary. Three approaches are possible:

1. derivatives of the Laplace transform of the FPT pdf;
2. solution of second order differential equations;
3. solution of the recursive formula proposed by Siegert ([130]).

Having the Laplace transform of the FPT pdf, one can compute:

$$ET^n = (-1)^n \frac{d^n g_\lambda(S|x_0)}{d(\lambda)^n} \quad (102)$$

where $g_\lambda(S|x_0)$ is given by (80). The presence of special functions in the Laplace transforms for the OU (36) or for the Feller processes (55) leads to very complex computations.

Alternatively, using the Kolmogorov equation and eq. (80), one can show that the moments of the FPT verify the recursive system of ordinary differential equations:

$$\sigma^2(x_0) \frac{d^2 ET^n(x_0)}{dx_0^2} + \mu(x_0) \frac{d ET^n(x_0)}{dx_0} = -n ET^{n-1}(x_0), \quad x_0 \in (l, S) \quad (103)$$

with boundary conditions:

$$ET^0(l) = 0, \quad ET^0(S) = 1. \quad (104)$$

When the process admits steady state distribution, one can write the solution of (102) through the Siegert formula (cf. [130]):

$$ET^n = t_n(S|x_0) = n \int_{x_0}^S \frac{2dz}{\sigma^2(z)W(z)} \int_l^z W(y) t_{n-1}(S|y) dy. \quad (105)$$

Due to the numerical difficulties of these formulae, in [84] approximations are proposed for specific processes (cf. Subsections 3.5 and 3.6) together with suggestions on the use of each one for specific ranges of the parameters.

4.1.5 Stochastic ordering

A further technique for the study of the FPT's is the stochastic comparison of the FPT's from different models (cf. [123], [118], [119]). Let us consider the FPT's T_1 and T_2 of two diffusion processes X_1 and X_2 over $I_1 = (l_1, r_1)$ and $I_2 = (l_2, r_2)$ with drifts $\mu_i(x)$, $x = 1, 2$ and diffusion coefficients $\sigma_i(x)$, $i = 1, 2$ respectively. Let the two processes Y_1 and Y_2 be obtained from X_1 and X_2 through the transformation

$$y_i = g_i(x) = \int_{l_i}^x \frac{dz}{\sigma_i(z)}, \quad i = 1, 2.$$

Moreover, let Y_1 and Y_2 verify the inequalities:

$$\mu_{Y_1}(y) \geq \mu_{Y_2}(y) \quad \forall y \in [0, g_2(S)]; \quad \frac{d\mu_{Y_2}(y)}{dy} \leq 0 \quad \forall y \in [0, g_2(S)] \quad (106)$$

and $\sigma_1^2(x) \geq \sigma_2^2(x)$.

For $x_0 \in (\max(l_1, l_2), S)$, $S \in (\max(l_1, l_2), \min(r_1, r_2))$, $x_0 < S$, it holds:

$$T_{X_1}(S|x_0) \leq_{as} T_{X_2}(S|x_0). \quad (107)$$

In (107), "as" means "almost surely". Note that Y_1 and Y_2 are characterized by unit diffusion coefficient and drift

$$\mu_{Y_i}(y) = \frac{1}{\sigma_i(x)} \left(-\frac{1}{4} \frac{d\sigma_i^2}{dx} + \mu_i(x) \right) \Big|_{x=g_i^{-1}(y)}. \quad (108)$$

4.1.6 Jump diffusion processes

The following integral equation for the FET pdf $\widehat{g}(S, t|y, \tau)$ of the process X in (68), defined over $I = [l, S]$ and originated in the state y at time τ , holds (cf. [50]):

$$\begin{aligned}
\widehat{g}(S, t | y, \tau) &= e^{-\lambda(t-\tau)} g(S, t | y, \tau) + \int_{\tau}^t du \int_l^S dz e^{-\lambda(u-\tau)} \\
&\times \{ \lambda^e f^a(z - a, u | y, \tau) + \lambda^i f^a(z + a, u | y, \tau) I_{(l, S-a)}(z) \} \\
&\times \widehat{g}(S, t | z, u) + \lambda^e e^{-\lambda(t-\tau)} \int_{S-a}^S dz f^a(z, t | y, \tau).
\end{aligned} \tag{109}$$

Here $\lambda = \lambda^e + \lambda^i$, $I_A(\cdot)$ is the indicator function of the set A , the jump amplitudes are $\delta^e = -\delta^i = a$. Furthermore $g(S, t | y, \tau)$ and $f^a(x, t | y, s)$ are the FPT and the transition pdf in the presence of the boundary S of the underlying diffusion process. The following approximate solution:

$$\begin{aligned}
\widehat{g}(S, t | y, \tau) &\approx e^{-\lambda(t-\tau)} g_t^S(y, \tau) + \lambda^e e^{-\lambda(t-\tau)} \int_{S-a}^S dz f^a(z, t | y, \tau) \\
&+ \lambda^e e^{-\lambda(t-\tau)} \int_{\tau}^t du \int_{-\infty}^{S-a} dz f_a(z, u | y, \tau) g_t^{S-a}(z, u) \\
&+ \lambda^i e^{-\lambda(t-\tau)} \int_{\tau}^t du \int_{-\infty}^S dz f^a(z, u | y, \tau) g_t^{S+a}(z, u) \tag{110}
\end{aligned}$$

holds (cf. [59]) for a Wiener process with drift μ and diffusion coefficient σ when $\lambda^e > \lambda^i$, $\lambda^e \ll 1$. Here $g_t^\xi(z, u) = g(\xi, t | z, u)$. This approximation can be interpreted in terms of sample path behavior for the process X . For jumps of low frequency, but relevant amplitude with respect to S , most of the sample paths cross the boundary either for diffusion without jumps or for an upward jump when $X_t \in [S - a, S)$ or for diffusion after at most a single (upward of downward) jump. The possible occurrence of a higher number of jumps is disregarded. Hence this approximation explains the first two peaks of the observed multimodal behavior exhibited by the FET pdf (cf. Fig. 4).

Some results on the moments of two simplified jump diffusion neuronal models are discussed in [50] and [51]. In the "large jumps" model the amplitude of exponentially time distributed jumps is large enough to determine a crossing of the threshold at each jump. Assuming that the crossing is a certain event, a recursive relation holds for the FET moments of order $n \geq 1$ of this model:

$$E[T^n] = \frac{n}{\lambda} \left\{ E[T^{n-1}] + (-1)^n \left[\frac{dg_{\lambda+\theta}^{(n-1)}(S|x_0)}{d\theta^{n-1}} \right]_{\theta=0} \right\}. \quad (111)$$

Here $g_{\lambda+\theta}(S|x_0)$ is the Laplace transform, of parameter $\lambda + \theta$, of the pure diffusion FPT, λ the frequency of jumps and the superscript (m) denotes the m -th derivative with respect to θ .

In the 'reset model' exponentially time distributed jumps force the membrane potential to return instantaneously to its resting level $V_R \equiv x_0$. Then the dynamics restarts anew till the crossing of the boundary or a new resetting. This model includes both upward and downward jumps of frequencies λ_1 and λ_2 , whose time epochs are described by means of two independent Poisson processes. One has:

$$\begin{aligned} E[T] &= \frac{1 - g_\lambda(S|x_0)}{\lambda g_\lambda(S|x_0)}; \\ E[T^2] &= \frac{2E[T]}{g_\lambda(S|x_0)} + \frac{2}{[g_\lambda(S|x_0)]^2} \left[\frac{dg_{\lambda+\theta}(S|x_0)}{d\theta} \right]_{\theta=0} \end{aligned} \quad (112)$$

with the notations as in (111) but $\lambda = \lambda_1 + \lambda_2$.

4.2 Numerical methods

4.2.1 The direct FPT problem

The direct FPT problem requires to determine the FPT pdf for a given process assuming the transition pdf and the boundary shape to be known. A large literature exists on numerical methods to solve the integral equations for the FPT pdf even for time not homogeneous diffusion processes (cf. [7], [14], [36], [39], [62], [103], [107]). The one proposed in [14] seems to be the fastest and most efficient. It consists in discretizing (86) when the function $k(t)$ is chosen to get a regular kernel for the second kind Volterra equation (cf. (88) or (89) for the OU and the Feller processes, respectively). Setting $t = t_0 + kh$, $k = 1, 2, \dots$, $h > 0$, the discretized solution of eq. (86) is

$$\begin{aligned}
\tilde{g}(S(t_0 + h), t_0 + h | x_0, t_0) &= -2\psi(S(t_0 + h), t_0 + h | x_0, t_0); \\
\tilde{g}(S(t_0 + kh), t_0 + kh | x_0, t_0) &= -2\psi(S(t_0 + kh), t_0 + kh | x_0, t_0) \\
&\quad + 2h \sum_{j=1}^{k-1} \tilde{g}(S(t_0 + jh), t_0 + jh | x_0, t_0) \\
&\quad \times \psi(S(t_0 + kh), t_0 + kh | S(t_0 + jh), t_0 + jh) \\
&\quad k = 2, 3, \dots
\end{aligned} \tag{113}$$

A suitable discretization step is necessary to make the numerical integration reliable. The numerical algorithm (114) uses previous integration steps to determine the successive values, hence it is important to get good evaluations on the first intervals. A heuristic rule is to execute at least twenty integration steps before the maximum of the FPT pdf occurs. In Fig. 7, panel A, we show the FPT pdf of a standard OU process with different integration steps. The error in the FPT pdf due to a wrong choice for h is enlightened in the evaluation of the FPT distribution (Panel B).

In [113] a strategy is proposed to solve numerically eq. (86) with an appropriate choice of the integration step. To this aim a time-dependent function, the FPT Location function, is introduced.

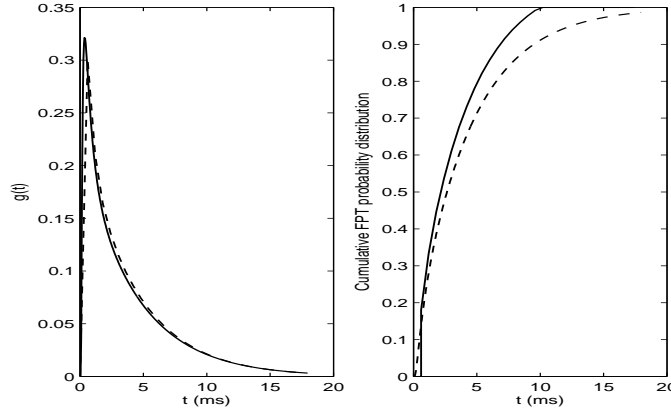


Fig. 7 FPT pdf (**panel A**) and FPT probability distribution (**panel B**) of an OU process obtained numerically with $\mu = 0 \text{ mVms}^{-1}$, $\sigma^2 = 1 \text{ mV}^2\text{ms}^{-1}$, $\theta = 1 \text{ ms}^{-1}$, $S = 1 \text{ mV}$; integration steps $h = 0.045$ (*continuous line*), $h = 0.6$ (*dashed line*)

4.2.2 The inverse FPT problem

The inverse FPT problem requires to determine the expression for the boundary $S(t)$ when the FPT pdf for a diffusion process is known, either in exact form or through a sample of FPT's. Two numerical algorithms are proposed to solve this problem for the Wiener process in [139] and extended to the OU process in [121]. The first algorithm proposes a Monte Carlo procedure to approximate the unknown boundary for the Wiener process stepwise. This algorithm is reliable and easily implemented but it is computationally expensive. The second approach, purely numerical, is computationally more attractive and extensions to processes different from the Wiener and the OU ones should hold. We present it here in the case of the Wiener process. By integrating Fortet's equation (79) in x from $S(t)$ to infinity (cf. [97]) one obtains the integral equation

$$\Psi\left(\frac{S(t)}{\sqrt{t}}\right) = \int_0^t \Psi\left(\frac{S(t)-S(s)}{\sqrt{t-s}}\right) g(s) ds \quad (t > 0) \quad (114)$$

where $\Psi(x) = 1 - \Phi(x)$, $\Phi(x) = \int_{-\infty}^x \varphi(z) dz$, $\varphi(z)$ is the standard normal pdf and $g(t) = g(S(t), t | x_0)$ is the FPT pdf for the Wiener process through the threshold $S(t)$. Equation (114) is a Volterra integral equation of the first kind in $g(s)$ but it is a non-linear Volterra integral equation of the second kind in $S(t)$. Its kernel is nonsingular since it is bounded. Moreover the functions involved in the equation are bounded and Ψ is invertible. Hence one can obtain numerically the approximate value $S^*(t_i)$ of $S(t_i)$ at the knots $t_i = ih$ for $i = 1, \dots, n$; here $h = t/n$ ($t > 0$ fixed). The integral on the l.h.s. of (114) is approximated by the Euler method:

$$\Psi\left(\frac{S^*(t_i)}{\sqrt{t_i}}\right) = \sum_{j=1}^i \Psi\left(\frac{S^*(t_i)-S^*(t_j)}{\sqrt{t_i-t_j}}\right) g(t_j) h \quad (i = 1, \dots, n), \quad (115)$$

getting a non-linear system of n equations in n unknowns $S^*(t_1), \dots, S^*(t_n)$. Note that the i -th equation, $i \geq 2$, makes use of the values $S^*(t_1), \dots, S^*(t_{i-1})$ in the preceding steps. Hence (115) can be solved iteratively to get approximate values for the unknown boundary S at the knots. The convergence of this algorithm and an estimate of its error are considered in [139].

Extensions to the case in which the FPT pdf is known only through samples of ISI's make use of the kernel method to approximate the FPT pdf (cf. [122]). Applications to neuronal modeling are proposed in [121] and [125] for the OU process. In particular in [125] this algorithm is employed to propose a classification method of groups of neurons when simultaneously recorded spike trains are available.

4.3 *Simulation methods*

In the study of neuronal models, when the process is not time homogeneous or the boundary is time dependent, the only available general technique is simulation. Despite its large use, this methods hides problems that may make the results for FPT's unreliable. The standard approach to the simulation of FPT's makes use of discretization algorithms for the SDE describing the membrane potential dynamics. Various reliable discretization schemes exist (cf. [74] and references quoted therein), depending on which degree of strong or of weak convergence is required. The easiest of these schemes is the so called Euler-Maruyama one (cf. **SUSANNE**).

The major cause of error in the simulation of FPT's is related to the chance to leave the crossing of the boundary undetected due to the discretization of the sample paths. Indeed a crossing happened inside the discretization interval results hidden in the discretized sample (cf. Fig. 8). This implies an important overestimation of the FPT, that does not disappear when the discretization step decreases (cf. [53]). The number of trials where the error may occur increases with the decrement of h , balancing the corresponding decrease in the probability of error.

Different solutions have been proposed to make the simulation of FPT's reliable. They suggest to evaluate the crossing probability during each integration step through the bridge process joining the last two values generated for the diffusion process. A bridge process $X^{[t_0, t_1]} = \{X_t^{[t_0, t_1]}, t \in [t_0, t_1]\}$ is associated to a given diffusion X by constraining X to take fixed values at the time instants t_0 and $t_1 > t_0$. The process $X^{[t_0, t_1]}$ is still a diffusion, since its sample paths are a subset of the set of sample paths of X .

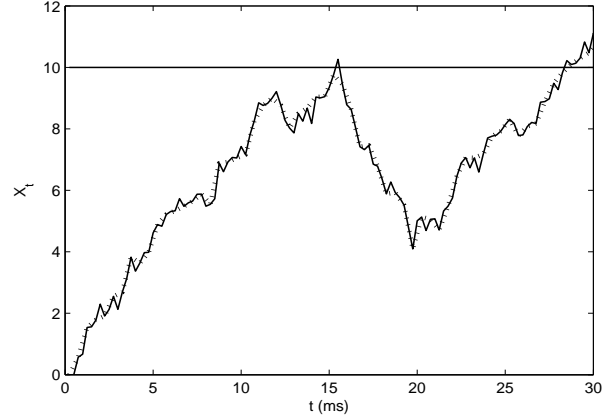


Fig. 8 A sample path of a diffusion process and its discretization. Exemplification of a missed crossing of the boundary inside a time interval of the simulation. *Circles*: simulated values of the sample path; *dots*: sample path

The crossing probability of the original diffusion during a simulation step, of amplitude h , coincides with that of its associated bridge on the same time interval (cf. for example [112]). Then one can evaluate, on each interval, the probability of hidden crossing for this process. For the Wiener process, the probability that the bridge $W^{[\tau, \tau+h]}$, originated in the state y at time τ and constrained to assume the value z at time $\tau + h$, crosses the boundary $S > y$ during $[\tau, \tau + h]$ is

$$P^* = P_W(S, h, y, z) = \exp \left\{ -\frac{2(S^2 - Sy - Sz + zy)}{2h\sigma^2} \right\}. \quad (116)$$

One can compare this value with a generated random number U uniform on $(0, 1)$ and, if $U < P^*$, conclude that a crossing has happened in that interval. The crossing probability of a Wiener process is used to approximate the crossing of the bridge associated to the process of interest in [66]. To introduce a more precise estimation of the crossing probability for the bridge we first recall the relationship between the transition pdf's $f(x, t | y, \tau)$ and $f^{[t_0, t_1]}(x, t | y, \tau)$ of the process X and of its bridge $X^{[t_0, t_1]}$ (cf. [112]):

$$f^{[t_0, t_1]}(x, t | y, \tau) = f(x, t | y, \tau) \frac{f(z, t_1 | x, t)}{f(z, t_1 | y, \tau)} \quad t_0 < \tau < t < t_1. \quad (117)$$

Denoting with $T^{[t_0, t_1]}$ the FPT of the bridge $X^{[t_0, t_1]}$ through the boundary S and with $g^{[t_0, t_1]}(S, t | x_0, t_0)$ its pdf it holds (cf. [39]):

$$g^{[t_0, t_1]}(S, t | x_0, t_0) = g(S, t | x_0, t_0) \frac{f(z, t_1 | S, t)}{f(z, t_1 | x_0, t_0)} \quad t_0 < \tau < t < t_1. \quad (118)$$

Integral equations analogous to (81) and (86) hold also for the FPT pdf of the bridge process. In [53] an approximate value of $g^{[t_0, t_1]}(S, t | x_0)$ is obtained, by disregarding the integral on the l.h.s of such equations. The approximation using eq. (86)

$$g^{[t_0, t_1]}(S, t | x_0, t_0) \cong -2\psi(S, t | x_0, t_0) \frac{f(z, t_1 | S, t)}{f(z, t_1 | x_0, t_0)} \quad (119)$$

produces very good estimates in the case of the OU and of the Feller underlying diffusion processes. In [53] the integral of this approximation over the discretization interval is used to estimate the probability of a hidden crossing inside each interval. In [55] a Monte Carlo algorithm is proposed to estimate the crossing probability of the bridge process. A numerical scheme is applied to the SDE for the bridge process to generate N samples. If L samples cross the boundary, the ratio L/N is used to estimate the crossing probability. The SDE for the bridge has drift and diffusion coefficients:

$$\mu^{[t_0, t_1]}(x, t) = \mu(x) + \frac{\sigma^2(x)}{f(z, t_1 | x, t)} \frac{\partial}{\partial x} f(z, t_1 | x, t); \quad \sigma^{[t_0, t_1]}(x) = \sigma(x) \quad (120)$$

respectively (cf. [55]). Here $\mu(x)$ and $\sigma^2(x)$ are the drift and the diffusion coefficient of the original diffusion X .

For a standardized OU process the coefficients (120) are (cf. [55]):

$$\mu_{OU}^{[t_0, t_1]}(x, t) = -x + \frac{2 [ze^{(t_1-t)} - x]}{[e^{2(t_1-t)} - 1]}; \quad \sigma_{OU}^{[t_0, t_1]}(x) = 1, \quad (121)$$

and for the Feller process are (cf. [55]):

$$\begin{aligned}
\mu_F^{[t_0, t_1]}(x, t) &= q + x \left[p - 2 \frac{pe^{p(t_1-t)}}{e^{p(t_1-t)} - 1} \right] \\
&\quad + \frac{2p\sqrt{xze^{p(t_1-t)}}}{e^{p(t_1-t)} - 1} \frac{I_{\frac{q}{r}} \left[\frac{2p\sqrt{xze^{p(t_1-t)}}}{r(e^{p(t_1-t)} - 1)} \right]}{I_{\frac{q}{r}-1} \left[\frac{2p\sqrt{xze^{p(t_1-t)}}}{r(e^{p(t_1-t)} - 1)} \right]} \\
\sigma_F^{[t_0, t_1]}(x) &= \sqrt{2rx}.
\end{aligned} \tag{122}$$

Here we employed the notation (51) and $I(\eta)$ denotes the modified Bessel function of parameter η .

A nested algorithm is proposed in [55] for the numerical solution of the SDE for the bridge. This choice avoids to evaluate the drift in $t = t_1$ where it becomes singular.

An alternative method to evaluate the hidden crossing probabilities, based on large deviation arguments, is proposed in [8]. This method is less precise than the previously mentioned ones but it does not request the knowledge of the transition pdf of the process X .

These algorithms can be applied also to jump diffusion processes but whenever a jump falls in between the two nodes t_n and t_{n+1} of the partition, the right end of the time interval $[t_n, t_{n+1}]$ should be substituted with the epoch \tilde{t}_n , $t_n < \tilde{t}_n \leq t_{n+1}$, of the jump event. To account for the possible hidden crossings inside the discretization intervals, the correction algorithm proposed in [53] should be employed.

A novel numerical method for the simulation of FPT has been recently proposed in [133]. The algorithm makes use of the representation of the stochastic process through an expansion using the Haar functions. It takes advantage of the dichotomic nature of this development to refine the description of the process in intervals where possible hidden crossings may arise.

In a recent paper [60] it is remarked that the membrane potential, until the spike, evolves in the presence of the boundary. The SDE for the process constrained by the boundary, i.e. for the process that has not yet attained the boundary till a fixed time, is determined. The SDE for its bridge, conditioned to cross the boundary for the first time at its right end, is also determined. Use of the simulation techniques allows to simulate these stochastic differential equations.

5 Estimation problems for LIF models

A few papers exist on the parameter estimation problem. The literature on this subject is rather recent, disregarding two oldest papers. The first one ([77]) considers a sample of membrane potential values observed at discrete times while [68] uses the moment method on a sample of ISI's. We focus here mainly on the available statistical methods for the OU and the Feller models. Their parameters can be divided into two groups: the intrinsic parameters, S, x_0, V_I and θ for the OU process and S, x_0, τ for the Feller process, and the input parameters, μ and σ^2 for the OU process and μ_F and σ_2^2 for the Feller one. The intrinsic parameters are often disregarded in estimation problems assuming their direct measure. In [63] the estimation of the refractory period is also discussed.

We distinguish in the sequel two types of methods, depending upon the available data:

1. Intracellular membrane recordings;
2. ISI time series.

5.1 Samples from membrane potential measures

In [85] a regression method and a maximum likelihood technique are applied to estimate $\beta = \frac{1}{\theta}$, μ and σ from intracellular data, supposed to follow an OU process. We report here the maximum likelihood estimators for the case of OU and Feller processes. One assumes that during an ISI the membrane depolarization $X_i = x_i$, $i = 0, 1, \dots, N$, is sampled at the $N + 1$ points $t_i = ih$. The maximum likelihood estimates are:

$$\hat{\beta} = \frac{1}{h} \frac{\sum_{j=0}^{N-1} x_j^2 - \sum_{j=0}^{N-1} x_{j+1}x_j + (x_N - x_0)\bar{x}}{\sum_{j=0}^{N-1} x_j^2 + \bar{x}^2 N}, \quad (123)$$

$$\hat{\mu} = \frac{x_N - x_0}{T} + \hat{\beta}\bar{x}, \quad (124)$$

and

$$\hat{\sigma} = \frac{1}{T} \sum_{j=0}^{N-1} \left(x_{j+1} - x_j + x_j h_j \hat{\beta} - h \hat{\mu} \right)^2 \quad (125)$$

where $\bar{x} = \frac{1}{N} \sum_{j=0}^N x_j$, $T = Nh$. The likelihood estimators $\hat{\mu}_F$ and $\hat{\alpha}$ for the parameters $\alpha = \frac{1}{\tau}$ and μ_F of the Feller process (cf. [12]) coincide with (123) and (124), while the estimator for σ_2^2 , putting $h_\Delta = \left(1 - e^{-\frac{\Delta}{\tau}}\right)$, is:

$$\hat{\sigma}_2^2 = \frac{2 \sum_{j=1}^N X_{i-1}^{-1} \left(X_i - \hat{\mu}_F \tau h_\Delta - X_{i-1} e^{-\frac{\Delta}{\tau}} \right)^2}{\sum_{j=1}^N X_{i-1}^{-1} \tau \left(\hat{\mu}_F \tau h_\Delta^2 + 2 X_{i-1} h_\Delta e^{-\frac{\Delta}{\tau}} \right)}. \quad (126)$$

Formulae (123) - (125) are obtained disregarding the existence of the firing boundary. This approximation determines a bias on the estimated values (cf. [9], [10]). The bias of the estimator of μ is of the same order of magnitude as the standard deviation of the estimate.

Unbiased estimators for μ are not yet available for the OU and the Feller models while the bias for the RRW and for the Wiener models are computed in a closed form in [9]. A comparative study on the estimators for the Feller process is performed in [10]. In [11] maximum likelihood estimators are derived from discrete observations of a Markov process up to the first-hitting time of a threshold, both in discrete and in continuous time. The models considered are the RRW, an autoregressive model of order one (AR(1)), and the Wiener, OU and Feller diffusions. For the last two ones approximations are introduced to evaluate the conditional transition pdf and the FPT distribution. These approximations hold when the sampling intervals are small. Their use allow to evaluate the likelihood function.

In [96] an algorithm is proposed to compute likelihoods, based on the numerical solution of the integral equation (86). Furthermore an estimator based on the large deviation principle is suggested to deal with the case of very small likelihoods in the tails of the distribution.

In [98] a maximum likelihood estimation method is employed for a particular LIF model with an additional variance parameter modeling possible slow fluctuations in the parameter μ .

In [67] a sample of discrete observations $X_{i\Delta}$, $i_0 \leq i \leq i_1$, $i_0 := \lceil \frac{t_0}{\Delta} \rceil$, $i_1 := \lceil \frac{t_1}{\Delta} \rceil$ of the process X of eq. (32), over the time interval $[t_0, t_1]$, is considered. The following nonparametric kernel estimators are proposed:

$$\begin{aligned}\widehat{\mu}(a) &= \frac{\sum_{i=i_0}^{i_1-M} K\left(\frac{X_{i\Delta}-a}{h}\right) \left(\frac{X_{(i+M)\Delta}-X_{i\Delta}}{\Delta M}\right)}{\sum_{i=i_0}^{i_1-M} K\left(\frac{X_{i\Delta}-a}{h}\right)} \\ \widehat{\sigma}^2(a) &= \frac{\sum_{i=i_0}^{i_1-M} K\left(\frac{X_{i\Delta}-a}{h}\right) \left(\frac{X_{(i+M)\Delta}-X_{i\Delta}}{\sqrt{\Delta M}}\right)^2}{\sum_{i=i_0}^{i_1-M} K\left(\frac{X_{i\Delta}-a}{h}\right)}\end{aligned}\quad (127)$$

with $h > 0$ a suitable bandwidth. Furthermore $K(y)$ may be chosen as a rectangular or triangular kernel, for a suitable integer M . Examples of possible kernels are $K(y) = \frac{1}{2}I_{\{-1,+1\}}(y)$ and $K(y) = (1 - |y|)I_{\{-1,+1\}}(y)$, with $I_{\{\bullet\}}(y)$ indicator function of the set $\{\bullet\}$.

Extensions to other processes and for the selection of the model (OU, Feller or different ones) are used to exemplify the method. The examples considered correspond to rarely spiking neurons, a fact that minimizes the problem underlined in [9], but prevents its use in other instances.

5.2 Samples of ISI's

The case of ISI data has been recently considered in [90]. In this paper an algorithm is proposed for computing maximum likelihood estimates with their confidence regions for μ and σ^2 . The algorithm numerically inverts the Laplace transform for the OU model. The method works also to estimate the parameter θ but it requests larger samples.

Maximum likelihood estimates for the OU model are obtained in [138] using numerical evaluations of (33). In [32] a variant of the moment method is proposed to estimate the input parameters of the OU process. In this paper an optimal stopping theorem is applied to determine the first two exponential moments of the FPT:

$$E\left(e^{T/\theta}\right) = \frac{\mu\theta}{\mu\theta - S}, \quad E\left(e^{2T/\theta}\right) = \frac{2(\mu\theta)^2 - \sigma^2\theta}{2(\mu\theta - S)^2 - \sigma^2\theta}. \quad (128)$$

The moment method is then applied to obtain the estimators $\widehat{\mu}_n$ and $\widehat{\sigma}_n^2$ from a sample of ISI's $\{T_1, \dots, T_n\}$:

$$\widehat{\mu}_n = \frac{S}{\theta} \frac{Z_{1,n}}{Z_{1,n} - 1}, \quad \widehat{\sigma}_n^2 = \frac{2S^2}{\theta} \frac{Z_{2,n} - Z_{1,n}^2}{(Z_{2,n} - 1)(Z_{1,n} - 1)^2} \quad (129)$$

where

$$Z_{1,n} = \frac{1}{n} \sum_{i=1}^n e^{T_i/\theta}, \quad Z_{2,n} = \frac{1}{n} \sum_{i=1}^n e^{2T_i/\theta}. \quad (130)$$

This method can be applied only in the suprathreshold region since the following conditions must be fulfilled: $E(e^{T/\theta}) < \infty$, $E(e^{2T/\theta}) < \infty$. The first condition is verified if $\mu\theta > S$ and the second holds if $\mu\theta > S$ and $\frac{\sigma^2\theta}{2} < (\mu\theta - S)^2$.

In [33] analogous results are proved for the Feller model, for which

$$E\left(e^{T/\tau}\right) = \frac{\mu_F\tau - y_0}{\mu_F\tau - S}, \quad E\left(e^{2T/\tau}\right) = \frac{(\mu_F\tau - y_0)^2 - \sigma_2^2\tau(\mu_F\tau/2 - y_0)}{(\mu_F\tau - S)^2 - \sigma_2^2\tau(\mu_F\tau/2 - S)}. \quad (131)$$

These expectations converge when $\mu_F\tau > S$ and $\frac{\tau\sigma_2^2}{2} \left(\sqrt{1 + \frac{2\mu_F}{\sigma_2^2}} - 1\right) < (\mu_F\tau - S)$. The estimators are:

$$\begin{aligned} \hat{\mu}_{F,n} &= \frac{S Z_{1,n} - y_0}{\tau Z_{1,n} - 1} \\ \hat{\sigma}_{2,n}^2 &= \frac{2(S - y_0)^2}{\tau} \frac{(Z_{2,n} - Z_{1,n}^2)}{[2(Z_{1,n} - 1)(SZ_{2,n} - y_0) - (SZ_{1,n} - y_0)(Z_{2,n} - 1)]}. \end{aligned} \quad (132)$$

Consistency and asymptotic normality of these estimators have been proved in [58]. The sample sizes required to get the asymptotic conditions are not huge (some hundreds), hence this property can be performed in neuronal experiments.

In [34] an alternative method to estimate μ and σ^2 , based on the analogous of (114) for the OU process,

$$\Phi\left(\frac{\mu\theta(1 - e^{-\frac{t}{\theta}}) - S}{\sqrt{\frac{\sigma^2\theta}{2}(1 - e^{-\frac{2t}{\theta}})}}\right) = \int_0^t g(u)\Phi\left(\sqrt{2}\frac{\mu\theta - S}{\sigma\sqrt{\theta}}\sqrt{\frac{1 - e^{-\frac{t-u}{\theta}}}{1 + e^{-\frac{t-u}{\theta}}}}\right) du, \quad (133)$$

is proposed. Numerical results suggest that this approach is preferable to the previous ones.

The case of observations of the trajectory on very short time intervals is considered in [95]. They propose a method to estimate the parameters of an OU process in this particular instance.

A recent review ([86]) has appeared summarizing the state of the art of the estimation problem for diffusion processes in neuromodeling instances. A comparison of the different estimation methods for the OU process is performed in [35].

Parallel spike trains are deeply discussed in [61]. This book presents the methods of correlation analysis together with a review on different approaches for the analysis of single spike trains. The different chapters discuss many important problems related with the statistical analysis of spike trains.

Finally the inverse FPT method is applied in [125] to classify simultaneously recorded spike trains. The value of the parameters for the OU process are assumed constant for all the recorded spike trains. The boundary is determined by the inverse FPT method and a comparison of the different boundaries is employed to classify the data.

The case of not stationary data is not contemplated by the estimation procedure. The problem of models whose noise term has a specific temporal structure has not been solved up to now. In [122] the inverse FPT method is used on samples of FPT's from an OU process to recover the boundary shape and to test nonstationary behaviors. The proposed method makes use of a moving window approach. The inverse FPT is applied on samples from each window. The comparison of the determined boundary shapes allows to detect changes in the observed dynamics.

References

1. Abrahams J., A survey of recent progress on level-crossing problems for random processes. In: Communications and Networks. A Survey of Recent Advances. (Blake I.F. and Poor H.V., eds.), 6-25. Springer-Verlag, New York (1986)
2. Abramowitz M. and Stegun I.A., eds. Handbook of Mathematical Functions with Formulas, Graphs, and Mathematical Tables, New York, Dover Publications (1972).
3. Albano G., Giorno V., Nobile A.G. and Ricciardi L.M. A Wiener-type neuronal model in the presence of exponential refractoriness, *BioSystems* 88): 202-215 (2007).

4. Albano G., Giorno V., Nobile A.G. and Ricciardi L.M. Modeling refractoriness for stochastically driven single neurons, *Sci. Math. Jpn.* 67(2): 173-189 (2008).
5. Alili L., Patie P. and Pedersen J.L. Representation of the First Hitting Time Density of an Ornstein-Uhlenbeck process, *Stochastic Models* 21: 967-980 (2005).
6. Alili L., Patie P. Boundary Crossing Identities for Diffusions having the Time-Inversion Property, *J. Theor. Probab.* 23: 65-84 (2010).
7. Anderssen R.S., DeHoog F.R. and Weiss R. On the numerical solution of Brownian motion processes. *J. Appl. Prob.* 10, 409-418 (1973).
8. Baldi P. and Caramellino L. Asymptotics of hitting probabilities for general one-dimensional diffusions. *Annals of Applied Probability*, 12, 1071-1095 (2002).
9. Bibbona E., Lánský P., Sacerdote L. and Sirovich R. Errors in estimation of input signal for integrate and fire neuronal models. *Physical Review E*, 78: Art. No. 011918 (2008).
10. Bibbona E., Lánský P. and Sirovich R. Estimating input parameters from intracellular recordings in the Feller neuronal model. *Physical Review E*, 81: Art. No. 031916. (2010).
11. Bibbona E. and Ditlevsen S. Estimation in discretely observed Markov processes killed at a threshold. Submitted (2010).
12. Bibby B. and Sorensen M. On estimation for discretely observed diffusions: A review. *Theory Stochastic Process.* 2, 49-56 (1996).
13. Brette R. and Gerstner W. Adaptive Exponential Integrate-and-Fire Model as an Effective Description of Neuronal Activity, *J. Neurophysiol.* 94, 3637-3642 (2005).
14. Buonocore A., Nobile A. G. and Ricciardi L. M. A new integral equation for the evaluation of the first-passage-time probability densities. *Adv. Appl. Prob.* 19, 784-800 (1987).
15. Buonocore A., Giorno V., Nobile A. G. and Ricciardi L. M. On the two-boundary first-crossing-time problem for diffusion processes. *J. Appl. Prob.* 27, 102-114 (1990).
16. Buonocore A., Caputo, L., Pirozzi, E. and Ricciardi L. M. On a Stochastic Leaky Integrate-and-Fire Neuronal Model. *Neural Computation* 22, 2558-2585 (2010).
17. Buonocore A., Giorno V., Nobile A.G. and Ricciardi L.M. A neuronal modeling paradigm in the presence of refractoriness, *BioSystems* 67, 35-43 (2002).
18. Burkitt A.N., A review of the integrate and fire neuron model: I. Homogeneous synaptic input. *Biol. Cybern.* 95, 1-19 (2006).
19. Burkitt A.N., A review of the integrate and fire neuron model: II. Inhomogeneous synaptic input and network properties. *Biol. Cybern.* 95, 97-112 (2006).
20. Capocelli R.M. and Ricciardi L.M. Diffusion approximation and first passage time problem for a model neuron. *Kybernetik* 8(6):214-23 (1971).
21. Capocelli R.M. and Ricciardi L.M. On the transformation of diffusion processes into the Feller process, *Math. Biosciences* 29, 219-234 (1976).
22. Cerbone G., Ricciardi L.M. and Sacerdote L. Mean Variance and Skewness of first passage time for the Ornstein-Uhlenbeck process. *Cyb. and Systems* 12, 395-429 (1981).

23. Chacron M. J., Longtin A., St-Hilaire M. and Maler L. Suprathreshold stochastic firing dynamics with memory in P-type electroreceptors. *Phys. Rev. Lett.* 85, 1576-1579 (2000).
24. Chacron M.J., Pakdaman K., Longtin A. Interspike interval correlations, memory, adaptation, and refractoriness in a leaky integrate-and-fire model with threshold fatigue *Neural Computation* Volume 15 , Issue 2 253 - 278 (2003).
25. Chacron M.J., Lindner B. and Longtin A. Threshold Fatigue and Information Transmission. *Journal of Computational Neuroscience* 23: 301-311 (2007).
26. Clopath C., Jolivet R., Rauch A., Luscher H.R. and Gerstner W. Predicting neuronal activity with simple models of the threshold type: Adaptive exponential integrate-and-fire model with two compartments, *Neurocomput.* 70: 1168-1673 (2007).
27. Cox D.R. and Miller H.D. *The Theory of Stochastic Processes*, Chapman & Hall (1977).
28. Daniels H. E. The minimum of stationary Markov process superimposed on a U-shaped trend. *J. Appl. Prob.* 6, 399-408 (1969).
29. Daniels H. E. Sequential tests constructed from images. *Ann. Stat.*, 10 , 394-400 (1982).
30. Di Crescenzo A. and Ricciardi L.M. On a discrimination problem for a class of stochastic processes with ordered first-passage-times. *Applied Stochastic Models in Business and Industry* 17: 205-219 (2001).
31. Di Crescenzo A., Di Nardo E. and Ricciardi L.M. On certain bounds for first-crossing-time probabilities of a jump-diffusion process. *Sci. Math. Jpn.* 64, no. 2, 449-460 (2006).
32. Ditlevsen S. and Lánský P. Estimation of the input parameters in the Ornstein-Uhlenbeck neuronal model. *Physical Review E* 71: Art. No. 011907 (2005).
33. Ditlevsen S. and Lánský P. Estimation of the input parameters in the Feller neuronal model *Physical Review E* 73: Art. No. 061910 (2006).
34. Ditlevsen S. and Ditlevsen O. Parameter estimation from observations of first-passage times of the Ornstein-Uhlenbeck process and the Feller process. *Probabilistic Engineering Mechanics*, 23: 170-179 (2008)
35. Ditlevsen S. and Lánský P.: Comparison of statistical methods for estimation of the input parameters in the Ornstein-Uhlenbeck neuronal model from first-passage times data. In *American Institute of Physics Proceedings Series, CP1028, Collective Dynamics: Topics on Competition and Cooperation in the Biosciences*, Eds.: L.M. Ricciardi, A. Buonocore, and E. Pirozzi (2008).
36. Durbin J. Boundary crossing probabilities for the Brownian motion and Poisson processes and techniques for computing the power of the Kolmogorov Smirnov test *J. Appl. Prob.* 8, 431-453 (1971).
37. Durbin J. The first-passage density of a continuous Gaussian process to a general boundary *J. Appl. Prob.* 22,1, 99-122 (1985).
38. Durbin J. and Williams D. The First-Passage Density of the Brownian Motion Process to a Curved Boundary *J. Appl. Prob.* 29,2, 291-304 (1992).

39. Favella L., Reineri M.T., Ricciardi L.M. and Sacerdote L. First-passage-time problems and some related computational methods. *Cyb. and Systems* 13, 95-128 (1982)
40. Fortet R. Les fonctions aléatoires du type Markoff associées à certaines équations linéaires au dérivées partielles du type parabolique *J. Math. Pure Appl.* (9) 22:177-243 (1943).
41. Gerstein G.L., Mandelbrot B. Random walk models for the spike activity of a single neuron, *Biophys. J.* 4,41-68 (1964).
42. Gerstner W. and Kistler W. M. *Spiking Neuron Models Single Neurons, Populations, Plasticity*, Cambridge University Press (2002).
43. Giorno V., Nobile A.G., Ricciardi L.M. and Sacerdote, L. Some remarks on the Raleigh process. *J. Appl. Prob.* 23, 398-408 (1986).
44. Giorno V., Lánský P., Nobile A.G. and Ricciardi L.M. Diffusion approximation and first-passage-time problem for a model neuron: III. A birth-and-death process approach. *Biol. Cybern.* 58, 387-404 (1988).
45. Giorno V., Nobile A.G. and Ricciardi L.M. A symmetry based constructive approach to probability densities for one dimensional diffusion processes *J. Appl. Prob.* 27, 707-721 (1989).
46. Giorno V., Nobile A.G., Ricciardi L.M. and Sato S. On the evaluation of first-passage-time probability densities via non-singular integral equations. *Adv. Appl. Prob.* 21, 20-36 (1989).
47. Giorno V., Nobile A.G. and Ricciardi L.M. On the asymptotic behavior of first-passage-time densities for one dimensional diffusion processes and varying boundary. *Adv. Appl. Prob.* 22, 883-914 (1990).
48. Giorno V., Nobile A.G. and Ricciardi L.M. Instantaneous return process and neuronal firings, in *Cybernetics and Systems Research 1992* (Trappl R. ,Ed.) World Scientific, 829-836 (1992).
49. Giorno V., Nobile A.G. and Ricciardi L.M., C. On the Moments of Firing Numbers in Diffusion Neuronal Models with Refractoriness. In: Mira, J., Alvarez, J.R. (Eds.), *IWINAC 2005. Lecture Notes in Computer Sciences 3561*, Springer-Verlag, 186-194 (2005).
50. Giraudo M.T. and Sacerdote L. Some remarks on First-Passage-Time for Jump-Diffusion Processes. *Cybernetics and Systems '96* (R. Trappl Ed.), University of Wien Press, Wien, p. 518-523 (1996).
51. Giraudo M.T. and Sacerdote L. Jump-diffusion processes as models for neuronal activity, *BioSystems* 40: 75-82 (1997).
52. Giraudo M.T. and Sacerdote L., Simulation methods in neuronal modeling. *BioSystems* 48:77-83 (1998).
53. Giraudo M.T. and Sacerdote L. An improved technique for the simulation of first passage times for diffusion processes *Communication in Statistics: simulation and computation.* 28, 4 (1999).
54. Giraudo M.T., A similarity solution for the Ornstein-Uhlenbeck diffusion process constrained by a reflecting and an absorbing boundary. *Ricerche di Matematica.* 49(1):47-63 (2000).

55. Giraudo M.T., Sacerdote L. and Zucca C. Evaluation of first passage times of diffusion processes through boundaries by means of a totally simulative algorithm. *Meth. Comp. Appl. Prob.* 3, 215-231 (2001).
56. Giraudo M.T., Sacerdote L. and Sirovich R. Effects of random jumps on a very simple neuronal diffusion model, *BioSystems* 67: 75-83 (2002).
57. Giraudo M.T., Sacerdote L. and Sirovich, R. Effects of random jumps on a very simple neuronal diffusion model, *BioSystems* 67: 75-83 (2002).
58. Giraudo M.T., Mininni R. and Sacerdote L. On the asymptotic behavior of the parameter estimators for some diffusion processes: application to neuronal models, *Ricerche di Matematica* 58 (1): 103-127 (2009).
59. Giraudo M.T. An approximate formula for the first-crossing-time density of a Wiener process perturbed by random jumps, *Statistics and Probability Letters* 79: 1559-1567 (2009).
60. Giraudo M.T., Greenwood, P.E. and Sacerdote L. How sample paths of Leaky Integrate and Fire models are influenced by the presence of a firing threshold. In press on *Neural Computation* (2011).
61. Grün S. and Rotter P. *Analysis of parallel spike trains*. Springer, New York (2010).
62. Gutierrez, R., Ricciardi, L.M., Román, P. and Torres, F., First-passage-time densities for time-non-homogeneous diffusion processes. *J. Appl. Prob.* 34, 623-631 (1997).
63. Hampel D, Lánský P: On the estimation of refractory period. *Journal of Neuroscience Methods*, 171: 288-295 (2008).
64. Helias M., Deger M., Diesmann M. and Rotter S.: Equilibrium and response properties of the integrate-and-fire neuron in discrete time. *Frontiers in Computational Neuroscience*, 3, Article 29 (2010).
65. Hodgkin A. and Huxley A. A quantitative description of membrane current and its application to conduction and excitation in nerve. *J. Physiol.* 117:500-544 (1952).
66. Honerkamp J. *Stochastic Dynamical Systems: Concepts, Numerical methods, Data Analysis*, VCH (1994).
67. Hopfner R. On a set of data for the membrane potential in a neuron *Math. Biosci.*, 207(2):275–301 (2007).
68. Inoue J, Sato S and Ricciardi LM. On the parameter estimation for diffusion models of single neuron's activities. I. Application to spontaneous activities of mesencephalic reticular formation cells in sleep and waking states. *Biol Cybern* 1995;73(3):209-221 (1995).
69. Jolivet R., Lewis T.J., and Gerstner W., Generalized Integrate-and-Fire Models of Neuronal Activity. Approximate Spike Trains of a Detailed Model to a High Degree of Accuracy, *J. Neurophysiol.*, 92(2):959–976 (2004).
70. Jolivet R., Roth A., Schurmann F., Gerstner W. and Senn W. Special issue on quantitative neuron modeling. *Biol. Cybern.* 99, 237-239 (2006).
71. Kallianpur G. On the diffusion approximation to a discontinuous model for a single neuron. *Contributions to statistics*, 247-258, North-Holland, Amsterdam, (1983).
72. Karlin S. and Taylor H. M. *A Second Course in Stochastic Processes*. Academic Press (1981).

73. Kistler W. M., Gerstner W. and vanHemmen J. L. Reduction of the Hodgkin-Huxley Equations to a Single-Variable Threshold Model, *Neural Comput.*, 9(5):1015–1045, (1997).
74. Kloeden P. and Platen P. *The numerical solution of Stochastic differential equations.* Springer (1992).
75. Kobayashi R., Tsubo Y. and Shinomoto S. Predicting spike times of any cortical neuron. *Frontiers in Systems Neuroscience. Conference Abstract: Computational and systems neuroscience.* doi: 10.3389/conf.neuro.06.2009.03.196 (2009).
76. Kobayashi R., Tsubo Y. and Shinomoto S. Made-to-order spiking neuron model equipped with a multi-timescale adaptive threshold. *Frontiers in Computational Neuroscience*, 3, Article 9 (2009).
77. Lánský P. Inference for the diffusion models of neuronal activity. *Mathematical Biosciences* 67:247-260 (1983).
78. Lánský P. and Lánská V. Diffusion approximations of the neuronal model with synaptic reversal potentials *Biol Cybern.* 56 , 19-26 (1987).
79. Lánský P. and Musila M. Generalized Stein’s model for anatomically complex neurons *Biosystems* 25, 179-191 (1991).
80. Lánská V., Lánský P. and Smith C.E. Synaptic transmission in a diffusion model for neural activity. *J Theor Biol* 166:393-406 (1994).
81. Lánský P., Sacerdote L. and Tomassetti F. (1996) On the comparison of Feller and Ornstein-Uhlenbeck models for neural activity. *Biol. Cybern.* 73, 457-465 (1995).
82. Lánský P. and Sato S. The stochastic diffusion models of nerve membrane depolarization and interspike interval generation. *Journal of Peripheral Nervous Systems* 4: 27-42 (1999).
83. Lánský P. and Rodriguez R. Coding range of a two-compartmental model of a neuron. *Biol. Cybern.* 81, 161 (1999).
84. Lánský P. and Sacerdote L. The Ornstein-Uhlenbeck neuronal model with signal-dependent noise. *Physics Letters A* 285, 132-140 (2001).
85. Lánský P., Sanda P., He J.F.: The parameters of the stochastic leaky integrate-and-fire neuronal model. *Journal of Computational Neuroscience* 21: 211-223 (2006).
86. Lánský P. and Ditlevsen S. A review of the methods for signal estimation in stochastic diffusion leaky integrate-and-fire neuronal models. *Biological Cybernetics* 99, 253-262 (2008).
87. Lapique, L. *Reserches quantitatives sur l’excitation électrique des nerfs traitée comme une polarization.* *J. Physiol. Pathol. Gen.* 9, pp. 620-635 (1907).
88. Lerche, H.R. *Boundary Crossing of Brownian Motion*, *Lecture Notes in Statistics*, Vol. 40, Springer-Verlag, Heidelberg-New York (1986).
89. Lindner B., Chacron M.J. and Longtin A. Integrate and fire neurons with threshold noise: A tractable model of how interspike interval correlations affect neuronal signal transmission *Physical Review E* 72, 021911 (2005).
90. Mullenowney P. and Iyengar Maximum Likelihood Estimation of an Integrate and Fire Neuronal Model. *Neural Computation.* 2008;20:1776-1795 (2007). *Neurocomputing* 32-33: 219-224 (2000).

91. Nobile A.G., Ricciardi L.M. and Sacerdote L. Exponential trends of first passage time densities for a class of diffusion processes with steady-state distribution. *J. Appl. Prob.* 22, 611-618 (1985).
92. Nobile A.G., Ricciardi L.M. and Sacerdote L. Exponential trends of Ornstein-Uhlenbeck first-passage-time densities. *J. Appl. Prob.* 22, 360-369 (1985).
93. Nobile A.G., Pirozzi E. and Ricciardi L.M. On the Estimation of First-Passage Time Densities for a Class of Gauss-Markov Processes EUROCAST 2007, M. Diaz ed. LNCS 4739, pp. 146-153 (2007).
94. Pakdaman K. and Mestivier D. (2001) External noise synchronizes forced oscillators *Phys. Rev. E* 64, 030901
95. Pawlas Z., Klebanov L.B., Prokop M. and Lánský P. Parameters of Spike Trains Observed in a Short Time Window. *Neural Computation*, 20: 1325-1343 (2008).
96. Paninski L., Haith A. and Szirtes G. Integral equation methods for computing likelihoods and their derivatives in the stochastic integrate and fire model. *J Comput Neurosci* (2008) 24:69-79 (2008).
97. Peskir, G. Limit at zero of the Brownian first-passage density. *Probab. Theory Related Fields* 124, 100-111 (2002).
98. Picchini U., Lánský P., De Gaetano A. and Ditlevsen S. Parameters of the diffusion leaky integrate-and fire neuronal model for a slowly fluctuating signal, *Neural Comput.* 20: 2696-2714 (2008).
99. Plesser H.E. and Diesmann M. Simplicity and efficiency of integrate-and-fire neuron models. *Neural Computation*, 21, 353-359 (2009).
100. Ricciardi L.M. On the transformation of Diffusion Processes into the Wiener process. *Journal of Mathematical Analysis and Applications* 54, 1: 185-199 (1976).
101. Ricciardi L.M. Diffusion Processes and Related Topics in Biology, Lecture Notes in Biomathematics, Vol. 14. Springer Verlag, Berlin (1977).
102. Ricciardi L.M. and Sacerdote L. The Ornstein-Uhlenbeck Process as a Model for Neuronal Activity, *Biol. Cybern.* 35, 1-9 (1979).
103. Ricciardi L.M., Sacerdote L. and Sato S. Diffusion approximation and first passage time problem for a model neuron II Outline of a computational method. *Math. Biosciences*, 64, 29-44 (1983).
104. Ricciardi L.M., Sacerdote L. and Sato S. On an Integral Equation for First-Passage-Time Probability Densities *Journal of Applied Probability*, Vol. 21, No. 2. pp. 302-314 (1984).
105. Ricciardi L.M. and Sato S. Diffusion processes and first-passage-time problems *Lectures Notes in Biomathematics and Informatics Ricciardi L.M. ed. Manchester Univ. Press* (1989).
106. Ricciardi L.M., Di Crescenzo A., Giorno, V. and Nobile A.G. On the instantaneous return process for neuronal diffusion models. In: *Marinaro, M., Scarpetta, G. (Eds.), Structure: from Physics to General Systems. World Scientific*, pp. 78-94 (1992).
107. Ricciardi L.M., Di Crescenzo A., Giorno V. and Nobile A. An outline of theoretical and algorithmic approaches to first passage time problems with applications to biological modeling. *Mathematica Japonica* 50 (2):247-321 (1999).

108. Ricciardi L.M., Esposito G., Giorno V. and Valerio C. Modeling neuronal firing in the presence of refractoriness. In: Mira, J., Alvarez, J.R. (Eds.), IWANN 2003. Lecture Notes in Computer Sciences 2686, Springer-Verlag, 1-8 (2003).
109. Rodriguez R. and Lánský P. Two-compartment stochastic model of a neuron with periodic input. Lecture Notes in Computer Science 1606 "Foundations and Tools for Neural Modeling (IWANN'99)", Springer Verlag (1999).
110. Rodriguez R. and Lánský P. A simple stochastic model of spatially complex neurons. *Biosystems* 58, 49 (2000).
111. Rodriguez R. and Lánský P. Effect of spatial extension on noise-enhanced phase locking in a leaky integrate-and-fire model of a neuron. *Physical Review E* 62, 8427 (2001).
112. Roger L.C.G. and Williams D. *Diffusions, Markov Processes and Martingales*. Wiley Series in Probability and Mathematical Statistics (1987).
113. Román P., Serrano J.J. and Torres F., First-passage-time location function: Application to determine first-passage-time densities in diffusion processes. *Computational Statistics and Data Analysis* 52, 4132–4146 (2008).
114. Sacerdote L. Asymptotic behavior of Ornstein-Uhlenbeck first-passage-time density through boundaries. *Applied Stochastic Models and Data Analysis*. 6, 53-57 (1988).
115. Sacerdote L., On the solution of the Fokker-Planck equation for a Feller process. *Adv. Appl. Prob.* 22(1):101–110 (1990).
116. Sacerdote L. and Ricciardi L.M. On the transformation of diffusion equations and boundaries into the Kolmogorov equation for the Wiener process. *Ricerche di Matematica* 41, 1: 123-135 (1992).
117. Sacerdote L. and Tomassetti F. On Evaluations and Asymptotic Approximations of First-Passage-Time Probabilities. *Adva Applied Probability*, Vol. 28, No. 1. pp. 270-284 (1996).
118. Sacerdote L. and Smith C.E. (2000) New Parameter Relationships Determined Via Stochastic Ordering for Spike Activity in a Reversal Potential Model. *BioSystem* 58: 59-65.
119. Sacerdote L. and Smith C.E. (2000) A qualitative comparison of some diffusion models for neural activity via stochastic ordering. *Biol. Cybernetics* 83, 6 543-551.
120. Sacerdote L. and Sirovich R. Multimodality of the interspike interval distribution in a simple jump-diffusion model *Scientiae Mathematicae Japonicae Online*, Vol. 8, 359-374 (2003).
121. Sacerdote L. and Zucca C. Threshold shape corresponding to a Gamma firing distribution in an Ornstein-Uhlenbeck neuronal model. *Scientiae Mathematicae Japonicae*. 58-2, 295-30 (2003).
122. Sacerdote L. and Zucca C. On the relationship between interspikes interval distribution and boundary shape in the Ornstein-Uhlenbeck neuronal model. *ECMTB Proceedings*. V. Capasso ed., 161-168 (2003).
123. Sacerdote L. and Smith C.E. Almost sure comparisons for first passage times of diffusion processes through boundaries. *Methodology and Computing in Applied Probability* 6, Number 3, 323-341 (2004).

124. Sacerdote L. and Sirovich R. Noise induced phenomena in jump-diffusion models for single neuron spike activity. IJCNN Proceedings, Budapest (2004).
125. Sacerdote L., Villa A.E.P. and Zucca C. On the classification of experimental data modeled via a stochastic leaky integrate and fire model through boundary values. Bull. Math. Biol. 68(6):1257-74 (2006).
126. Sato S. Evaluation of the First-Passage Time Probability to a Square Root Boundary for the Wiener Process, J. Appl. Prob. 14 (4): 850-856 (1977).
127. Sato S. Note on the Ornstein-Uhlenbeck process model for stochastic activity of a single neuron, Lecture Notes in Biomath, 70: 146-156 (1987).
128. Segundo J., Vibert J.-F., Pakdaman K., Stiber M. and Diez Martinez O. Noise and the neuroscience: a long history, a recent revival and some theory. In: Pribram, KH eds. , Origins: brain & self organization, Erlbaum, Hillsdale, NJ (1994).
129. Shimokawa T., Pakdaman K. and Sato S. Time-scale matching in the response of a leaky integrate-and-fire neuron model to periodic stimulus with additive noise, Phys. Rev. E 59, 3427 3443 (1999).
130. Siegert A.J.F. On the First Passage Time Probability Problem, Phys. Rev. 81, 617–623 (1951).
131. Sirovich R. Mathematical models for the study of synchronization phenomena in neuronal networks, Ph. D. Thesis, University of Torino and Université de Grenoble (2006).
132. Stein R.B. A theoretical analysis of neuronal variability, Biophys. Journal 5, 385-386 (1965).
133. Taillefumier T. and Magnasco M.O. A Fast Algorithm for the First-Passage Times of Gauss-Markov Processes with Hölder Continuous Boundaries, J. Stat. Phys. 140: 1130–1156 (2010).
134. Tuckwell H. C. Introduction to theoretical neurobiology. Volume 1. Linear cable theory and dendritic structure, Cambridge University Press, Cambridge, UK (1988).
135. Tuckwell, H. C. Introduction to theoretical neurobiology. Volume 2. Introduction to theoretical neurobiology, Cambridge, UK:Cambridge University Press (1988).
136. Uhlenbeck G.E. and Ornstein L.S. On the theory of Brownian motion, Phys. Rev. 36, 823-841 (1930).
137. Wang L. and Potzelberger K. Boundary crossing probability for Brownian motion and general boundaries, J. Appl. Prob. 34: 54-65 (1997).
138. Zhang X., You G., Chen T. and Feng J. K. Maximum likelihood decoding of neuronal inputs from an interspike interval distribution, Neural Computation 19 (4), 1319-1346 (2009).
139. Zucca C. and Sacerdote L. On the Inverse First-Passage-Time Problem for a Wiener Process Annals of Applied Probability, In press (2009)